2006

Effects of ultra violet and visible light on bacterial survival / by Natasha Vermeulen.

Vermeulen, Natasha

The Effects of Ultra Violet and Visible Light on Bacterial Survival

Author: Natasha Vermeulen
M.Sc. Candidate Biology
2006-31-08
Supervisor: Dr. Kam Leung
Co. Supervisors: Dr. Werden Keeler, Dr. Kanavillil Nandakumar

Your file Votre référence
ISBN: 978-0-494-31202-5
Our file Notre référence
ISBN: 978-0-494-31202-5

Abstract of the Thesis

The optical dose in mJ/cm^2 for causing mortality of *Escherichia coli*, using wavelengths between 230-375 nm in the UV and 400-532 nm in the mid-visible spectral regions, has been determined in this study. Currently, the mercury 254 nm UV line or UV flash lamp sources are used in most optical equipment designed for bactericidal action. However, little is known about the bactericidal effect of UV at longer than 254 nm and visible light radiation between 400-532 nm. An accurate knowledge of the bactericidal dose versus wavelength is of central importance in the optimal choice of light source for a given application. Now that UV diodes and lasers emitting in the 280 to 340 nm range are entering the developmental phase, they can be added to the list of existing UV flash lamps, discharge lamps and high intensity visible lasers for use in bactericidal applications.

E. coli cell suspensions at about $1x10^8$ CFU/ml were exposed to various dosages of radiation between 230-532 nm and the survival cell densities were determined by drop-plating. Radiation between 260 to 280 nm in the UV region was most efficient in killing the *E. coli* cells. In addition, significant mortality of *E. coli* was observed when the cell suspensions were exposed to visible light at 458 and 488 nm. Based on the *E. coli* survival data at various wavelengths and dosages, we constructed a predictive equation to estimate the survival of *E. coli* when exposed to a known dosage of radiation at a specific wavelength. $\text{Log}(S/S_o) = -(1.089 \times 10^7 e^{-0.0633\lambda})D$

Where S = survivor cell density (CFU/ml),

S_o = initial cell density (CFU/ml),

D = Radiation dose (mJ/cm^2),

λ = wavelength of radiation (nm).

It was also determined that *E. coli* cells had an absorption peak between 260-280 nm which coincided with the UV spectrum that had the highest killing capacity for *E. coli*.

The FTIR spectrums of UV-treated and untreated *E. coli* showed that there was a decrease of C-O-C and C-O-P bondings after the UV treatment, indicating the destruction of the glycan backbone of peptidoglycan and phosphodiester backbone of nucleic acids, respectively. There was also an increase in protein content in the UV-treated samples because there was a significant increase in the amide bonds. This increase may be a stress response mechanism of the *E. coli* cells exposed to the UV treatment. The UV-treated cells also showed an increase in the amount of CH_2 stretching of fatty acids, indicating a change in membrane structure of the UV treated cells. Furthermore, UV-treated samples showed an increase of hydroxyl functional group, an indication of an increase of reactive oxidation species (ROS) in the *E. coli* cells.

Acknowledgements

The author would like to thank all of my supervisors and co-supervisors, Dr. Werden Keeler, Dr. Kam Tin Leung, and Dr. Kanavillil Nandakumar for all the help they provided during this research. I am grateful for all the help Dr. Kam Tin Leung provided me throughout my thesis and valuable suggestions he gave me throughout my research work. In addition, I would like to thank Dr. Kanavillil Nandadumar who has given me useful tips throughout my work and for all the editorial work he as assessed me with. I would like to particularly thank Dr. Werden Keeler for the use of his Physics lab and all the valuable work he has done in order to help me with my research. I would also like to thank Dr. Heidi Schraft for all the help and tips she has given me throughout my work.

This study was funded by a Natural Science and Engineering Research Council of Canada (NSERC) Discovery Grant.

Table of Contents

List of Figures

List of Tables

Chapter 1: Literature Review

1.1 Introduction

Ultraviolet (UV) radiation damages many living organisms including prokaryotic bacteria, lower and higher plants, animal tissues and fungi (Hockberger, 2002). UV is and has been used for many purposes, including waste and drinking water treatment (Decho, 2000), blood irradiation (Ben-Hur and Petrie, 2004), operating room disinfectant, to sterilize operating instruments and as a bactericidal agent (Wilson, 1994). In addition, there has been extensive research on the destructive mechanisms of UV on cells (Godley et al., 2005; Hader and Sinha, 2005; Becerra et al., 2004).

Currently, the mercury 254nm UV line or UV flash lamp sources are used in most optical equipment designed for bactericidal purposes (Decho, 2000; Sharrer et al., 2004; Schwartz et al., 2003). However, longer wavelength at mid-visible light can induce bacterial mortality if the dose is high enough (Godley et al., 2005; Hamblin et al., 2005). Now that UV diodes and lasers emitting in the 280nm to 340nm range are entering the development phase, they can be added to the list of existing UV flash lamps, discharge lamps and high intensity visible lasers for use in bactericidal applications. Thus, accurate knowledge of the bactericidal dose versus wavelength is of central importance in the optimal choice of light source for a given application.

Conversely, little is known about the lethal effects of visible light on microorganisms and there is even less known on the killing mechanisms of visible light. Visible light lasers are being used for photodynamic therapy (Szpringer et al., 2004) to remove dental plaque and are being looked into as a possible bactericidal agent (Wilson, 1994). More information is needed to assess whether visible light alone could

affect bacterial mortality and thus it could be more accepted as a possible way to treat infections. With modern visible lasers as light sources, implementing the use of visible light in the control of microorganisms could be cost effective. In addition, there may be fewer side effects for the patient than modern drugs.

This study is a spectral analysis from 230 to 532 nm, which aims to determine the effects UV and visible light have on bacteria mortality. With a partial goal to determine the effectiveness of visible light has on killing bacteria. Generating such information has broad applications in the medical, environmental, and physical fields. An *Escherichia coli* strain was selected to be a bacterial model to test the disinfecting properties of UV and visible light. This bacterium was chosen because it is an indicator of fecal contamination in drinking water and has pathogenic forms that affect the health of people world wide (Deborah Chen and Frandel, 2005).

1.2 Overview of Ultraviolet and Visible Light

Ultraviolet (UV) and visible light are components of the electromagnetic spectrum (Cartier, 2004). Visible light is the only portion of the electromagnetic spectrum that the human eye can see. Visible radiation precedes infrared light on the electromagnetic spectrum, ranging from about 400 to 700 nm (Jones and Childers, 1993). If a white light is passed though a prism, a color spectrum will be noticeable. This color spectrum includes violet, blue, cyan, green, yellow, orange and red light (Crummett and Westem, 1994). After visible light on the electromagnetic spectrum, UV radiation is predominant (Jones and Childers, 1993).

UV light, ranges from 10 nm to about 400 nm, and is more energetic than visible light (Crummett and Westem, 1994). There are three categories of UV, UVA (320nm - 400nm), UVB (290nm-320nm) and UVC (below 290) (Cartier, 2004). Indoor tanning beds use UVA emissions. UVB is predominately the tanning agent when outdoors, and UVC gets absorbed by the atmosphere. UV irradiation has been accepted as a highly effective way to kill microorganisms for decades (Jagger, 1976; Hockberger, 2002). UV has also been used to kill yeast, viruses and fungi (Devine et al., 2001).

1.3 Past and Present Research on the Effects Ultraviolet Irradiation on Bacteria

In the 18th century, it was believed that sunlight, in the form of sunbaths, cured many ailments, such as skin ulcers and other skin anomalies (Hokberger, 2002). Ward (1884) reported that on plate cultures, *Bacillus anthracis* spores where killed by sunlight and not by increasing temperature. At one time, it was recommended that sunlight disinfection of drinking water should be implemented. Research then evolved into looking at how UV irradiation could be used for sanitation, disinfection, and sterilization (Hokberger, 2002).

Gates (1929), exposed *Staphylococcus aureus* to varying, wavelengths (238nm to 302nm), intensities, times, and examined the lethal action of UV on this bacterium. It was found that *S. aureus* was killed by UV, but the rate at which the bacteria were killed was dependent on different energy levels at different wavelengths. However, in order to achieve total kill of this bacterium, long exposure times were needed. It was noted that this might be due to the speculation that young bacteria are more resistant to UV light than that of the older bacteria. Thus, it was thought that the resistance of these young

bacteria increased exposure time. A second paper, written by Gates in 1929, indicated that trying to study wavelengths higher than 302nm was faulty because the amount of exposure time needed was unrealistic and such an exposure time may be prone to many uncertainties. Also, temperature change was measured in his study and it was stated that change in temperature was not high enough to induce mortality in *S. aureus*. A third study by Gates (1930) showed that within the wavelengths used (238-302nm), lower dose was needed between 260-270nm in order to generated significant kill than any other wavelengths tested. This peak in bactericidal action was speculated to correlate with the absorption spectrum of *S. aureus*, where there is a peak of light absorption between 260-270nm. However, it was stated that experimental errors accosted with obtaining the absorption spectrum for *S. aureus* where numerous, thus rendering such data unreliable. Preceding these studies, there seems to be no other notable studies investigating the dose dependence and wavelength relationships of UV killing. Increasingly more interest was put into the mechanisms of UV killing.

In the 1970s, research was being done in order to understand how UV induces growth and division delay in *E. coli* (Thomas, 1977). DNA damage was thought to be the prime suspect for UV induced bacterial impairment (Eisenstark, 1987). The mechanisms of UV action are detailed later in this review.

A study by Folwaczny et al. (1998) used a 308nm laser to determine the bactericidal effects it had on *S. aureus* and *E. coli*. The laser produced a significant reduction in bacterial cells at an energy density of 0.5 J/cm^2. It was also noted that the temperature change noticed was only 4.5°C higher than the original temperature of the sample, which was significantly below the critical temperature increase that would result

in thermal damage. In a similar study, Richter et al. (2002) used a pulsed nitrogen laser at a wavelength of 337nm on a biofilm forming bacterium *E. coli*. At a fluence of 0.74 J/cm^2, the removal of the biofilm was observed.

1.3.1 Applications of Ultraviolet Disinfection

The disinfectant properties of UV irradiation can be implemented in numerous ways that are currently being used for medical and industrial practices. Such practices include using UV as an operating room and medical instrument disinfectant (Wilson, 1994), for drinking water and waste water treatment (Decho, 2000).

UV irradiation has been used in operating rooms for more than a half of a century, so to reduce airborne bacterial infections (Lidwell, 1994). Due to the use of UV as an operating room disinfectant, there has been a substantial reduction in the incidence of wound sepsis or deep sepsis due to joint replacements (Lowell and Pierson, 1989).

UV irradiation is used in conjunction with other disinfectants as an effective way to treat bacterial communities that contaminate waste water (Schwartz, 2003). Some waste water treatment plants employ UV disinfectant techniques exclusively, dismissing the use of chemicals, and thus the possible harmful side effects they might have. Excluding the use of other harmful chemicals like chlorine, UV as a disinfectant can reduce the pollution in aquatic systems. It is also well documented that chlorine can produce by-products that are mutagenic (Chang et al., 1985). UV can also be used as a sterilizing agent in hospitals and other facilities that require procedures to disinfect equipment. The use of UV irradiation as an antiseptic might have implications in treating some human ailments.

UV irradiation could, also, be implemented as an effective way to treat human illnesses without the use of light sensitive drugs. An example of this is the use of UV blood irradiation to kill viruses, such as hepatitis C, AIDS and bacteria. UV blood irradiation is used by first draining blood from the patient, mixing the blood with an anticoagulant, then exposing it to a selected UV dose and then returning the treated blood back into the patient (Ben-Hur and Petrie 2004). Ben-Hur and Petrie (2004) noted that patients that used this technique showed a 66 to 96 percent reduction of the hepatitis C virus titer in their blood. This study also states that the patent with the 96 percent reduction of hepatitis C could possibly be on his/her way to recovery. Excluding the use of light sensitive drugs, UV irradiation would be a cheep and effective way of treatment.

1.3.2 Present Understanding of the Lethal Mechanisms Associated with Ultraviolet Irradiation

UV irradiation, between 100nm and 400nm, is known to denature the DNA of microorganisms, resulting in bacteria mortality (Sharrer et al., 2005). When bacteria are exposed to UV the formation of free radicals become more predominant, these chemicals then interfere with DNA transcription and replication, thus, leading to the eventual misreading of the genetic code. This causes mutations and possible death of the cells (Sinha and Hader, 2002). UV radiation also induces harmful effects on important molecules such as proteins, lipids, and chromophores (Hader and Sinha, 2005). Single and double DNA strand breaks are, also, thought to be an important cause of cell death (Jagger, 1976).

UV damage can also affect the cytoplasmic membrane of bacterial cells. It has been shown that when *E. coli* is exposed to UV light, considerable damage to the membrane is noticeable (Eisenstark, 1987). Membrane damage could further degrade the cell, with DNA injury, making repair mechanisms less successful. However, it is commonly known that DNA degradation is the major factor effecting bacterial mortality due to UV irradiation (Weber, 2005; Moan, 1989).

Bacteria exposed to UV light causes the production of free radicals, such as the reactive oxygen species (ROS) (Heck, 2003; Hader and Sinha, 2005; Wei et al., 1998). The production of ROS can cause DNA, RNA, protein and lipid damage, producing altered cell growth and differentiation (Wei et al., 1998). There are three main types of ROS, which are the superoxide anion, hydrogen peroxide and singlet oxygen (Becerra et al., 2004). DNA double-strand breaks are one of the major products of ionizing radiation and ROS (Tuteja and Tuteja, 2001). Single strand breaks and double strand breaks are, also, thought to decrease as wavelength increases (Moan, 1989).

In addition, less energetic UV radiation causes chemical modification in DNA, resulting in different DNA lesions. These DNA lesions can change a coding base into a mutagenic one or a lethal non-coding lesion (Hader and Sinha, 2005). There are two main DNA lesions caused by UV radiation, which are cyclobutane-pyrimidine dimers (CPDs) and pyrimidine (6-4) pyrimidone photoproducts (6-4PPs) and their Dewar valence isomers (Sinha and Hader, 2002). CPDs and 6-4PPs block the function of DNA and RNA polymerases, which may in turn result in the misreading of nucleotides or may inhibit polymerase progression during DNA replication or transcription (Weber, 2005). CPDs are the most abundant mutagens present after UV disinfection and thought to be

the most cytotoxic lesion. However, the 6-4PPs may inflict more serious and mutagenic effects (Sinha and Hader, 2002). Buger et al. (2002) found that some *E. coli* cells, after UV irradiated, lost their ability to divide and this dysfunction may be due to the formation of CPDs.

1.3.3 UV Repair Mechanisms

Mutations arise due to DNA damage by UV irradiation, which in turn can be repaired, but without repair the mutant cells can show malignant transformations. To combat the effects of UV irradiation many organisms utilize different repair mechanisms to maintain genetic integrity and prolong life.

One major repair mechanism that can to minimize the effects of UV damage is the enzyme DNA photolyases. Discovered in 1993, DNA photolyases are monomeric proteins that repair the lethal and carcinogenic effects of UV (Carell et al., 2001). There are two major types of DNA photolyases, one that repairs CPDs called CPD photolyases and one that fixes 6-4PPs called (6-4) photolyases (Carell et al., 2001). CPD photolyases have been found in bacteria, fungi, plants, invertebrates and many vertebrates. Photolyase is dependent on blue light excitation in order to reverse DNA damage due to UV light (Hader and Sinha, 2005).

Excision repair, on the other hand, does not rely on light activation and is referred to as a dark repair pathway. This pathway is complex and works by replacing damaged DNA with new nucleotides based on the information on the complementary strand (Hader and Sinha, 2005). Excision repair is divided into two categories, which are base excision repair (BER) and nucleotide excision repair (NER). BER is thought to protect cells from the ROS hydrolysis and the simple alkylating agents, utilizing key enzymes

called DNA glycosylases (Tuteja and Tuteja, 2001). There are specific DNA glycosylases that remove different types of damage, and the repair pathway is determined by the kind of glycosylase involved. With a total of 30 gene products, NER repairs many types of DNA lesions, including CPDs and (6-4)PPs (Sinha and Hader, 2002).

Another important mechanism that cells use to fix derogated DNA is recombination repair, which effectively restores double-strand DNA breaks and single-strand DNA gaps. This is done through a process of complex biochemical reactions that utilize varying numbers of gene products (Sinha and Hader, 2002). DNA Repairs after UV irradiation are not foolproof, the repairs might cause errors that change the genetic script of the microorganisms, causing mutations and flawed replication.

1.4 Review and Present Research on the Effects of Visible Light on Bacteria

Visible light is less energetic than UV light, and thus is a less effective disinfectant. Early research into the killing effects of visible light left most scientists skeptical about the validity of such work. It was unknown weather the killing action was due to other reasons, such as the possible UV or heat emitted by the lamps used (Eisenstark, 1971). However, it has been shown that, with the right dose of energy, visible light will kill bacteria (Hamblin et al., 2005).

Earlier research into the killing properties of visible light was used for treatments in plaque-related diseases or as a disinfectant in the dental field. Extra-oral bacterial species, such as *Pseudomonas aeruginosa* and *Staphylococcus aureus* where being treated with laser light and killed (Wilson, 1994).

Hamblin et al. (2005) conducted an experiment where they showed that visible light alone can kill *Heliobacter pylori* in the stomach of humans, using fiber optics. The wavelength of light that was most useful in killing this bacterium was between 375nm-475nm with a dose of 100mW/cm^2. A study conducted by Elman et al. (2003) noted that after exposing *acne vulgaris* to 405-420nm UV free blue light, a significant reduction of this bacterium was noticed.

Nandakumar et al. (2003) used a Nd:YAG laser at 532nm, with a fluence of 0.1 J/cm^2, to irradiate two coastal water diatoms, *Chaetoceros gracilis* and *Skeletonema costatum*. It was found that the visible laser induced significant mortality in both *S. costatum* and *C. gracilis*. Furthermore, Nandakumar et al. (2002) also used the same Nd:YAG laser to asses the mortality of *Pseudoalteromonas carrageenovora*. After 15 minutes of irradiation on the bacterium, counts went down 53%. It was also found that mortality of the bacterium increased as the duration of laser irradiation increased. In addition, after 5 hours of the laser treatment, the total viable count of the bacteria decreased 87.14 to 99.01%. Another study by Nandakumar et al. (2003) showed that visible laser at 532nm was very effective in removing *Pseudoalteromonas carrageenovorsa* biofilm. More information is needed in order to assess whether visible light could kill harmful bacteria and if so at what energy and dose levels.

1.4.1 Applications of Visible Light for Anti-Cancer and -Microbial Therapies

Photodynamic therapy (PDT) is a relatively new technique that strives to kill cancer cells using visible light sources and light sensitive drugs. PDT utilizes the generation of free radicals, due to light irradiation, to harm and possibility kill the cancer

cells being treated (Moore et al., 2005). Treatments that use PDT are becoming more of an acceptable standard. This therapy has been approved for use by the U.S. Food and Drug Administration and various other organizations throughout the world (Dougherty, 2002). PDT has been used, successfully, to treat gram-negative and gram-positive bacteria, mycoplasma, fungi, viruses, and various infectious diseases (Hamblin et al., 2005). This new procedure has also been used to treat human patients with different malignant, premalignant and ophthalmic conditions and is also being investigated for the treatment of localized infections in humans (Szpringer, 2004).

1.4.2 Present Knowledge on the Lethal Mechanisms of Visible Light

Little is known about how visible light affects microorganisms, even though some studies have shown that certain wavelengths of visible light can cause cellular inactivation and cell death (Godley et al., 2005). Eisenstark (1987) noted that UVA and visible light produce biological damages on bacteria cells, different from that of UVB, and UVC. In the visible region, it is thought that the majority of DNA damage is caused by single strand DNA cleavage (Moan, 1989). The use of high power visible lasers can cause photochemical effects, such as the breaking of chemical bonds, which in turn could also affect the mortality of bacterial cells (Nandakumar et al., 2003).

Research into how visible light, up to 700nm, affects cell mortality indicates that damage is primarily caused by reactive oxygen species (ROS) (Hader and Sinha, 2005; Godley et al., 2005). These include singlet oxygen, hydroxyl radical and superoxide anion (Godley et al., 2005). The generation of excess ROS can damage lipids, proteins, and DNA. Godley et al. (2005) showed that blue light irradiation on non-

pigmented epithelial cells cause mitochondrial dysfunction and mtDNA damage. However, no measurable damages were found on nuclear DNA. This implied that mitochondrial DNA was more susceptible to ROS damage.

Another theory describing how bacteria are sensitive to visible light is that many species of bacteria are fluorescent, and thus more responsive to specific wavelengths of visible light. Furthermore, it has been shown that some bacteria may have some natural photosensitizers, such as porphyrins, cytochromes, and carotenoids, which make the bacteria more sensitive to certain wavelengths (Hamblin et al., 2005). Some studies have also shown that visible light irradiation can cause a reduction of NADH (Eisenstark, 1971) and ATP (Nandakumar et al., 2003) in bacterial cells.

1.5 Using the Attenuated Total Reflectance - Fourier Transform Infrared (ATR-FTIR) to Study UV Damages on Bacterial Cells

UV-induced damages to bacterial cells can be measured by determining the increase in H_2O_2 (a product of superoxide anion) or 8-hydroydeoxyguanosine (generated by oxidative damage of DNA) (Schriner et al., 2005). However, these assays are designed to quantify specific groups of UV affected chemicals that indicate specific types of UV damage. Therefore, these assays cannot reflect the effect of UV on the overall changes in bacterial cells at the molecular level. The FTIR can be used to analyze the types and the relative amount of biochemical bonds in a complex organic sample and the resulting IR spectrum represents a molecular fingerprint of the sample (Hirschmugl, 2004). FTIR analysis is well suited for examining the overall impact of UV radiation on bacterial cells at the molecular structure level. One of the objectives of this study is to examine the effect of UV damage at the molecular level of *E. coli* cells.

The ideas that lead to FTIR spectroscopy started with the invention of the Michelson interferometer, created by Albert Abraham Michelson in 1880 (Griffiths, 1986). The FTIR spectrometer, however, was not commercially available until the 1940s and the technology then was far from what it is today (Stuart, 1996).

FTIR spectroscopy is useful in the analyzing a variety materials, such as liquids, pastes, films, solutions, powders, films, gases, fibers and many different kinds of solid surfaces (Stuart, 1996). It provides data on chemical bondings between atoms and is based on the vibrations of atoms and bonds in a molecule or molecular system (Hirschmugl, 2004).

1.5.1 Bond Vibrations

When interpreting infrared spectra, it is important to note that peaks in an IR spectrum correspond to bond vibration modes of a specific molecule. Thus, it is important to understand the concept of bond vibrations.

Bond vibrations include bond stretching (i.e. change in bond length) and bond bending (i.e., change in bond angle) (Smith, 1996). Stretching of bonds can vary, some stretch symmetrically, while others stretch asymmetrically (Hirschmugl, 2004). Bending vibrations can be in or out of a plane, including deformations, rocking, wagging, and twisting (Christy et al. 2001). Deformations occur when certain atoms in a molecule move in opposite directions of its plane, and rocking happens when atoms move in the same direction in its plane (Hirschmugl, 2004). Wags and twists are vibrations out of a particular plane. Within a particular molecule, there may be many different modes of

vibrations. For example, alkyl bromide (CH_2=$CHCH_2Br$) has 21 vibration modes (Smith, 1996).

1.5.2 Attenuated Total Reflectance (ATR)

An ATR accessory is used to hold a sample in place for the FTIR analysis. Usually, samples can be in form of solid, liquid, semisolid or thin film samples (Smith, 1996). In the centre of the ATR accessory, there is an infrared transparent crystal of high refractive index, such material can be zinc selenide (ZnSe), KRS-5 (thallium iodide/thallium bromide) or germanium (Smith, 1996). In addition, there is an accessory that mounts over the crystal that compresses the sample to ensure that the surface contact is optimal (Griffiths, 1986).

ATR is achieved by placing a sample on an infrared transmitting crystal of ZnSe in our case. The crystal has the shape of the bottom half of a regular prism and light is fed into and out of it at the sloped ends. Since it has a larger refractive index than the sample, the infrared light that enters the prism is internally reflected at the interface between the prism and the sample (Christy et al., 2001). Total internal reflection occurs when the angle of incidence at the interface between the sample and crystal is greater then the critical angle (Stuart, 1996). Although total internal reflection implies that light does not leave the crystal, there is a short distance beyond the crystal surface (~$\lambda/4$) termed the evanescent region, that optical energy penetrates. When material is pressed into this region, its optical spectrum can be obtained.

1.6 *Escherichia coli*

E. coli is a Gram - negative bacterium and a natural part of the gut flora in humans. Thus, most *E. coli* strains are not harmful to humans and other mammals. However, some *E. coli* strains are pathogenic and cause severe illness in humans (Betts, 2000). Such illnesses include urinary tract infection, diarrhoeal illness, hemorrhagic colitis, hemorrhagic uremic syndrome (Kuhnert et al., 2000), dysentery, bladder infections, pneumonia, septicemia, and meningitis (Salyers and Whitt, 2002). A well documented serotype of this bacterium is *E. coli* 0157: H7. This serotype is a well known as a food poisoning organism which only requires a small amount to be ingested in order to case illness (Betts, 2000).

Despite the fact that most *E. coli* strains are non-pathogenic, the presence of this bacterium in drinking water treatment facilities or in commercial foods indicates feacal contaminations and potential existence of feacal pathogens. Thus, *E. coli* is used as a fecal contamination indicator to assess the cleanliness of drinking water and commercial foods (Van Houdt and Michiels, 2005). When the total number of *E. coli* in a sample is quantified, a risk assessment of the sample can be determined based on the *E. coli* density (Kuhnert et al., 2000).

1.7 Objectives

The objectives of this study are to: (i) evaluate the disinfection properties of UV and visible light on an *E. coli* strain ATCC 25922; (ii) develop a predictive equation to estimate the killing capacity of various wavelengths of radiation at different dosages;

and (iii) develop an ATR-FTIR spectroscopic method to study the effect of UV radiation on the *E. coli* strain at the molecular level.

Chapter 2: Broad Spectrum Analysis of UV and Visible Light on *E. coli*

2.1 Introduction

Ultraviolet (UV) and visible light are part of the electromagnetic spectrum (Cartier, 2004). Ultraviolet light is invisible to the human eye; visible light, on the other hand, is the only portion of the electromagnetic spectrum the human eye can see. Visible light ranges from about 400nm to 700nm, where as UV radiation starts at 10nm and proceeds until roughly 400nm (Jones and Childers, 1993). UV light is more energetic and has shorter wavelengths then visible light, thus penetrates water poorly (Crummett and Westem, 1994). Conversely, visible light is less energetic, but penetrates water better than UV radiation, because wavelengths of visible light are longer (Jones and Childers, 1993).

UV light has been documented to be effective in damaging many living organisms such as prokaryotic bacteria, eukaryotic cells, lower and higher plants, animal tissues and fungi (Hockberger, 2002). There are many important uses for UV disinfection, including waste and drinking water treatment (Decho, 2000), blood irradiation (Ben-Hur and Petrie, 2004), operating room disinfectant, to sterilize operating instruments and as a bactericidal agent (Wilson, 1994). UV blood irradiation is used by first draining blood from the patient, mixing the blood with an anticoagulant, then exposing it to a selected UV dose and then returning the treated blood back into the patient (Ben-Hur and Petrie 2004). Ben-Hur and Petrie (2004) noted that patients that used this technique showed a 66 to 96 percent reduction of the hepatitis C virus titer in

their blood. In order to carry out the disinfecting properties of UV irradiation the mercury 254nm UV line is used in most UV bactericidal systems. However, with the creation of new UV diodes and lasers, emitting radiation between 280nm to 340nm, applying this new technology to UV flash and discharge lamps can create a whole new line of bactericidal applications with greater penetrability than the 254nm line.

There is little known on the lethal effects of visible light, however visible light lasers are being used as bactericidal agents, for photodynamic therapy (Szpringer et al., 2004), and to remove dental plaque (Wilson, 1994). Photodynamic therapy (PDT) is a relatively new technique that strives to kill cancer cells using visible light sources and light sensitive drugs (Moore et al., 2005). The use of visible light as a bactericidal agent may prove to be cost effective and cause fewer side effects then modern drugs. Hamblin et al. (2005) showed that visible light alone can kill *Heliobacter pylori* in the stomach of humans, using fiber optics. The wavelength of light that was most useful at killing this bacterium was between 375 and 475 nm with a dose of 100mW/cm^2. Due to the fact that visible light is less energetic than UV, it has been questioned whether it can be used as a bactericidal agent. Hence, more information is needed in order to assess whether visible light could kill harmful bacteria and if so at what energy dosages.

The bacterium *Escherichia coli* is used to determine the bactericidal effects of UV and visible light. *E. coli* is a gram negative bacterium and is a natural part of the human gut flora. Thus, most *E. coli* strains are not harmful to humans or other mammals. However some *E. coli* strains are pathogenic and can cause severe illness in humans (Betts, 2000). Such illnesses include urinary tract infection, diarrhoeal illness, hemorrhagic colitis, hemorrhagic uremic syndrome, dysentery, bladder infections,

pneumonia, septicemia, and meningitis (Salyers and Whitt, 2002). These harmful strains of *E. coli* can leach out into the environment (due to fecal contamination) and become present in human food and drinking water (Kuhnert et al., 2000). Thus, *E. coli* is used as an indicator organism to assess the cleanliness of drinking water and commercial food (Van Houdt and Michiels, 2005). The total number of *E. coli* can be quantified, in a sample and a risk assessment can be determined based on this number (Kuhnert et al, 2000).

The purpose of this study is to examine the mortality of *E. coli* ATCC 25922 when it is exposed to radiation at different wavelengths (250-532 nm) and dosages. The second objective is to develop a predictive model to estimate the killing capacity of various wavelengths of radiation at different dosages.

2.2 Materials and Methods

2.2.1 UV Source

The light source, though a monochromator, was a 100W PTI xenon arc lamp. A Jarrell- Ash ¼ meter monochromator was used to select the wavelength of light under study (Figure 2.1). The wavelengths selected where 230nm, 240nm, 250nm, 265nm, 275nm, 290nm, 300nm, 325nm, 350nm, 365nm, and 375nm. Each wavelength had varying doses and the dose was measured using a pyroelectric power meter (Laser Precision Corp., Utica, New York).

2.2.2 Laser Sources

The visible light source consisted of two types of lasers. For wavelengths 457.9nm, 488nm and 514nm, a Coherent Innova 70.4 Argon Ion laser was used (Figure

2.2). The Argon Ion laser lines were separated by a glass prism. The power output of this laser was 700mW at 488nm and at 457.9nm. At 514 nm the output of the Argon Ion laser was two watts. At 532 nm, a Spectra Physics Mellenia V frequency doubled Nd:YAG laser (Figure 2.2) was used. Light intensity of the Nd:YAG laser was measured at 2.0W. Dose and power output was measured by a Coherent 210 laser power meter (measured 0-100W).

2.2.3 Bacteria Preparation

The *E. coli* ATCC 25922 strain, a Gram-negative bacterium, were obtained from the American Type Culture Collection (ATCC). It was stored in 25% glycerol at -80°C, and re-grown on tryptic soy agar plates. The *E. coli* cells were cultured in tryptic soy broth for 15h, in a shaking incubator at 100*rpm*, at 37°C. After incubation, the medium was washed in sterile distilled water and centrifuged for 10 minutes at 3000 x *g*. This process was repeated three times. An OD of 0.30 was selected for both UV and visible light treatments. The *E. coli* suspension was placed in a device used for either UV or visible light exposure.

2.2.4 UV Treatment

As soon as the *E. coli* was prepared in suspension, 100µl of the cell suspension was pipetted into a device used for UV treatment (Figure 2.3). This device was composed of a glass slide with an aluminum ring; this ring was affixed on the glass slide with nail polish (Figure 2.3). In addition, the aluminum ring was tapered along the center so that the shadowing of the suspended medium will be negligible. After 100µl of *E. coli* suspension is put into the aluminum ring, the device was put under a Jarrell-Ash ¼ meter monochromator. When the appropriate UV wavelength was selected, the *E.*

coli suspension was treated with a selected dose. After treatment, the medium was serial diluted and drop plated.

2.2.5 Laser Treatment

An *E. coli* suspension, 1ml, was put into a 4ml glass cuvette with a small magnet stir bar at the bottom. This device was placed on a magnetic stir plate. During visible light irradiation the liquid culture was stirred with the bar magnet. For treatment, an Argon Ion laser or a frequency double Nd:YAG laser was used. After treatment, 100µl was taken out of the treated *E. coli* suspension and serial diluted and drop plated.

2.3 Results

2.3.1 Effect of UV and Visible Radiation on E. coli

Figure 2.1 to 2.19 show the killing capability of radiations at various wavelengths, ranging from 230-532 nm. Between 265-532 nm a higher dosage of radiation was required to cause morality of *E. coli* at a longer wavelength (Figure 2.20). However, when the wavelength of the UV was below 265 nm, the killing capacity of the radiation also decreased. At 265 nm, the UV radiation was most effective in killing the *E. coli* cells, requiring about 1.17 log mJ/cm^2 to achieve 100% killing. However, a higher dosage of UV radiation was required to reach 100% killing when the *E. coli* cells were exposed to radiation with a wavelength shorter than 265 nm (Figure 2.22). For instance, at 230 nm and 300 nm, radiation dosages of 1.80 and 1.95 log mJ/cm^2 were required to cause 100% morality of the *E. coli* cells.

Radiations in the visible spectrum, such as 400, 458 and 488 nm were able to kill the *E. coli* cells and a one-log reduction of the *E. coli* cells were observed at about 4.2, 5.5 and 6.9 log mJ/cm^2, respectively (Figure 2.21). However, visible radiations with

wavelengths longer than 500 nm did not cause any significant reduction on the viability of the *E. coli* cells when the dosage of radiation was < 7 log mJ/cm^2.

2.3.2 Analysis of Bacterial Survival vs. Applied Optical Dose

All of the UV and visible light dose dependent survival curves could be fit using the equation $y = P_1 - P_2 e^{(P3 \cdot x)}$. Initially, the parameters P_1, P_2 and P_3 were adjustable best fit parameters. However, P_1 is just the y-intercept of the survival curve. Since this was always normalized to an initial *E. coli* sample number of 7.85 (expressed as a log unit), P_1 must also be 7.85 for all values of λ. P_2 determines the degree of bending of each curve, and this was dependent on the radiation wavelength. During the fitting process, it was noted that P_3 was always a value near 2.3. Since 2.3026 is the factor for converting log to ln, it was eventually set to this constant for all the equations.

Noting that 'y' is the log of the survivor number (log S), 'x' is the logarithm of the optical dose (log D) in mJ/cm^2, and $P_1 = \log S_o = 7.85$, we have for P_3 a parameter

$$\boxed{\log S = \log S_o - P_2 e^{(P3 \cdot x)}} \qquad \text{Equation 2.1}$$

or $\log S = \log S_o - P_2 \cdot e^{(P3 \cdot \log D)}$

$\log S = \log S_o - P_2 e^{[(P3 \cdot (\ln D)/2.3026]}$

$\log S = \log S_o - P_2 e^{[\ln(D) \cdot P3/2.3026]}$

so $\log S = \log S_o - P_2 D^{P3/2.3026}$

But since it was found that P_3 was always close to 2.3026

$$\boxed{\log S = \log S_o - P_2 D} \qquad \text{Equation 2.2}$$

Thus, we have the general form

$$\boxed{\log (S/S_o) = - P_2 D} \qquad \text{Equation 2.3}$$

At the 100% lethal dose level, D_{lethal}, the survival number (i.e. log S) is zero, and from Equation (2.2)

$$\log S_o = P_2 D_{lethal}$$

So the expression for the lethal radiation dose at a given wavelength, is

$$D_{lethal} = 7.85/P2 \quad \text{or} \quad \log(D_{lethal}) = \log(7.85/P2) \qquad \text{Equation 2.4}$$

2.3.3 Wavelength Dependence of P_2

Based on Figure 2.24 the relationship between log P_2 and λ can be represented by an linear equation of the form $y = y_o + mx$ i.e. as

$$\log P_2 = A + B\lambda.$$

From a linear best fit using Origin 7.0, one obtains $A = 7.0369 \pm 0.4134$ and $B = -0.0275 \pm 0.00117$.

The above equation can be rewritten as:

$$\log P_2 = \log K - b\lambda \log(e) \qquad \text{where } B = -b \log(e) \text{ and } \log K = A$$

or $$P_2 = Ke^{-b\lambda}$$

Therefore:

$$K = 1.0886 \times 10^7 \qquad \text{with an uncertainty of } \sim 6\%$$

Since log e = 0.43429 and B = -0.0275

$$b = -B/\log(e) = 0.0275 \pm 0.00117 / 0.43429 = 0.0633 \pm 0.00269$$

Thus, in terms of wavelength λ, and leaving out the uncertainties of about 6%

$$P_2 = 1.089 \times 10^7 e^{-0.0633\lambda} \qquad \text{Equation 2.5}$$

Incorporating P_2 into the original survivor equation 2.3 for S, finally results in:

$$\boxed{\text{Log}(S/S_o) = -(1.089 \times 10^7 e^{-0.0633\lambda}) D} \qquad \text{Equation 2.6}$$

This form shows the exponential relation between survivors S and D, and the double exponential relation between S and λ.

2.3.4 UV and Visible Light Absorption Spectrum of E. coli

The absorption spectrum of the *E. coli* suspension (Figure 2.23) shows that the absorbance of the sample increases with the decrease of wavelength of the incident radiation. However, an absorption peak was observed at 265 nm before the absorbance increased exponentially at wavelengths less than 240 nm.

2.3.5 Wavelength and Bond Breaking Energy Equivalence

The energy required to break covalent bonds in biological systems (kcal/mole) can be converted to the equivalent wavelength in nanometers needed to break certain bonds in a biological system (Table 2.2). Examples of these conversions are explained below:

Energy Conversions:

1 mole = 6.023×10^{23} items

1 calorie = 4.186 joules

1 joule = 1 coulomb x 1 volt

Since the charge on an electron or proton has magnitude ~1.6×10^{-19} coulomb, if it is moved through a potential difference of 1 volt, the energy change is 1 electron-volt (eV). This leads to the more convenient small scale energy unit of the electron-volt (eV).

So: 1eV = 1.60217×10^{-19} joules

Using the conversion factors above,100 kcal/mole in eV/item (where items = photons) becomes:

100 x (4,186joule/6.02217 x 10^{23} items) x (1eV/1.60217 x 10^{-19} joule) = 4.3384 eV/item.

The energy of a photon in eV can also be determined from:

$E = h\nu = hc/\lambda$ where ν = photon frequency, c = speed of light, and

λ = wavelength, and h = Planck's constant

Substituting h = 6.626068 x 10^{-34} joule-sec and setting c = 2.99792458 x 10^{14} microns/sec, for λ in microns gives:

$E(eV) = 1.23984/\lambda(\mu m)$.

From the above, 100 kcal/mole bond energy is 4.3437 eV per bond and the equivalent photon wavelength for this energy is:

$\lambda(\mu m) = 1.23984/4.3437 = 0.28559\ \mu m = 285.35$ nm.

These conversions indicate that UV – visible photons represent enough energy to effectively break strong bonds in biological systems. Photons of the various characteristic bond energies strike a biological system, bonds should be broken or at least altered quickly in either a direct manner or through induced reactions.

Tables

Table 2.1

P_2 parameter fits for all wavelengths studied, with associated error numbers.

Wavelength λ	Single P_2 parameter fits*	Log(P_2)	Log(P_2) error
230	0.1252	-0.90239	±0.01214
250	0.27451	-0.56144	±0.03228
265	0.52329	-0.28125	±0.0276
275	0.44537	-0.351323	±0.0199
290	0.27691	-0.55766	±0.04556
300	0.08587	-1.06616	±0.02895
325	0.00509	-2.29328	±0.05521
350	0.00245	-2.6108	±0.01907
365	0.00265	-2.57675	±0.0819
375	0.00234	-2.63078	±0.01817
400	0.00006	-4.2218	±0.06695
458	3.37E-6	-5.47237	±0.06182
488	1.5106E-7	-6.82086	±0.10913

* $P_2 = [(1.089 \pm 0.4134) \times 10^7)] \exp -(0.0633 \pm 0.0027)\lambda$

Table 2.2

Type of bond broken with a specific energy in kcal/mole, eV/bond, or specific photon wavelengths. The color associated with photon wavelengths is also included.

Bond	Energy (kcal/mole)	Energy (eV/bond)	Photon Wavelength (nm)	Colour
O - H	110	4.7722	259.80	grey
H - H	104	4.5119	274.79	grey
P - O	100	4.3384	285.78	grey
C – H	99	4.2520	291.58	grey
N - H	93	4.0347	307.29	grey
C - O	84	3.6442	340.22	grey
C - C	83	3.6009	344.32	grey
S - H	81	3.5141	352.82	grey
C - N	70	3.0369	408.26	violet
C - S	62	2.6898	460.94	blue-violet
N - O	53	2.2994	539.21	green
S - S	51	2.2126	560.36	yellow

Figures

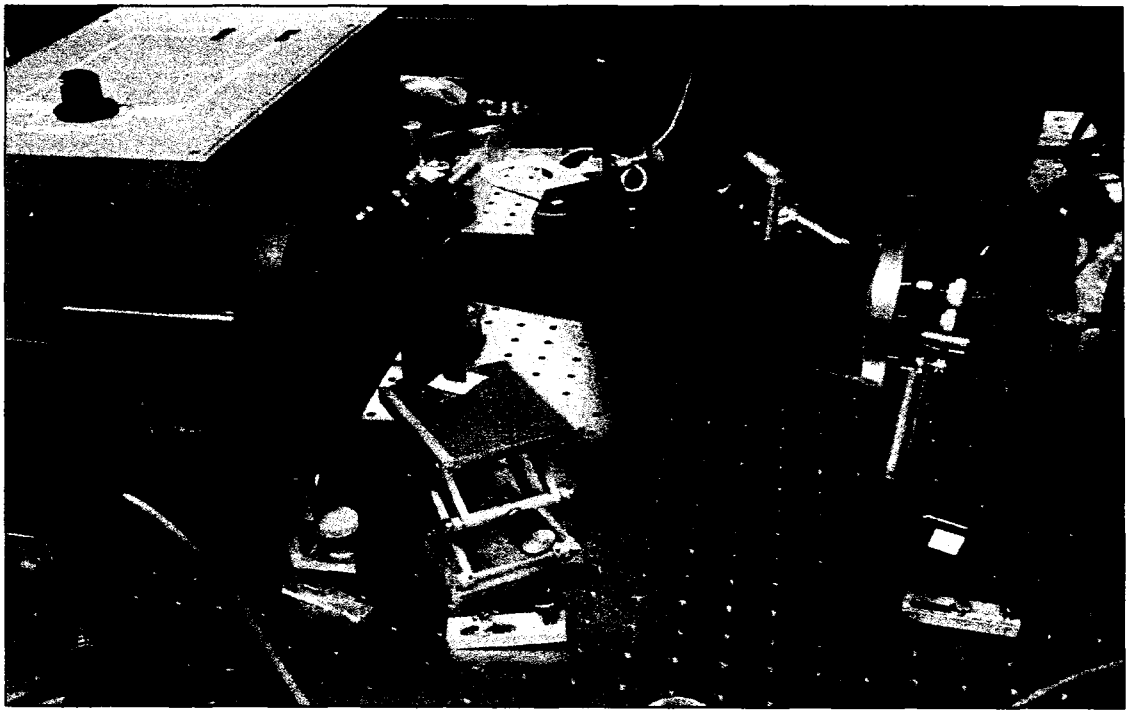

Figure 2. 1 - UV output from the monochromator redirected onto the sample.

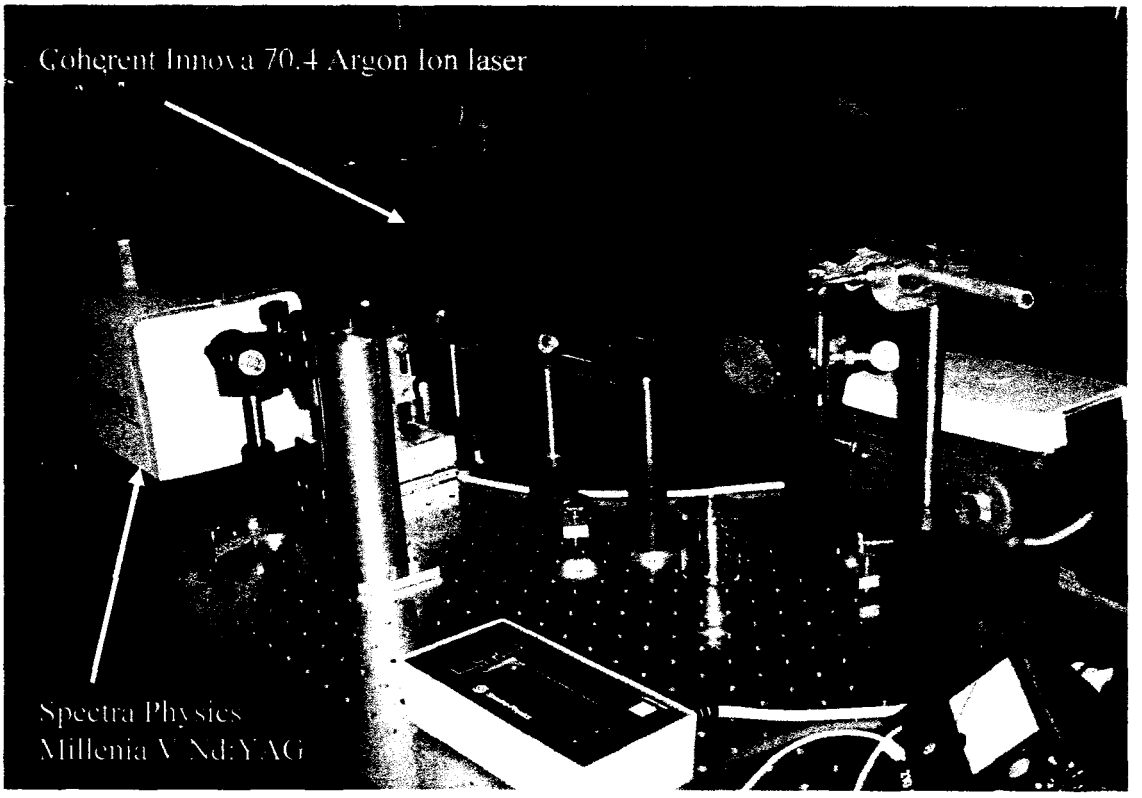

Figure 2. 2 - A Coherent I-70, 4 watt Argon Ion laser for 457.9nm, 488nm and 514nm illumination. Also, a Spectra Physics Millenia V frequency doubled Nd:YAG laser for 532nm illumination.

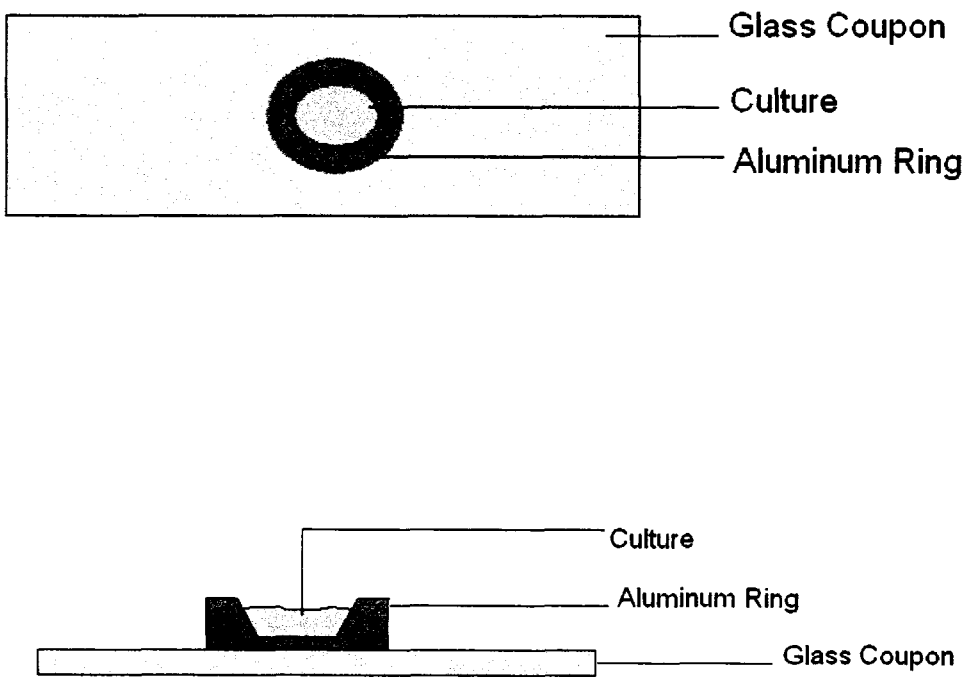

Figure 2. 3 - Sample holder used for UV radiation in planar and lateral views.

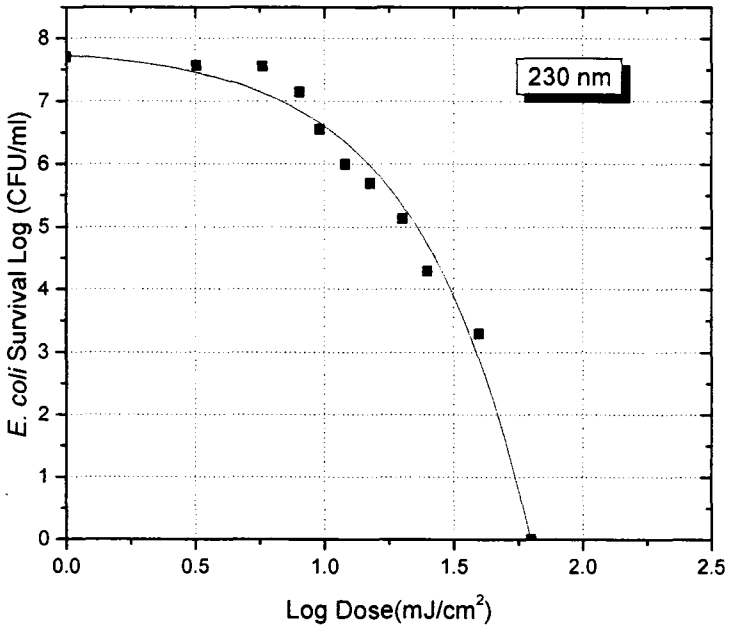

Figure 2. 4 - *E. coli* log survival vs. log dose at 230nm. Parameter P_2 = 0.1252.

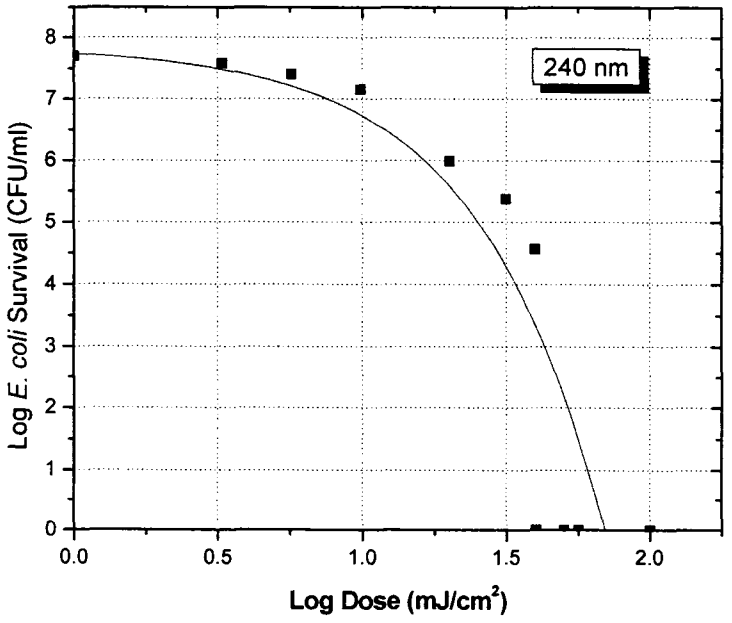

Figure 2. 5 - *E. coli* log survival vs. log dose at 240nm, with P_2=0.11279.

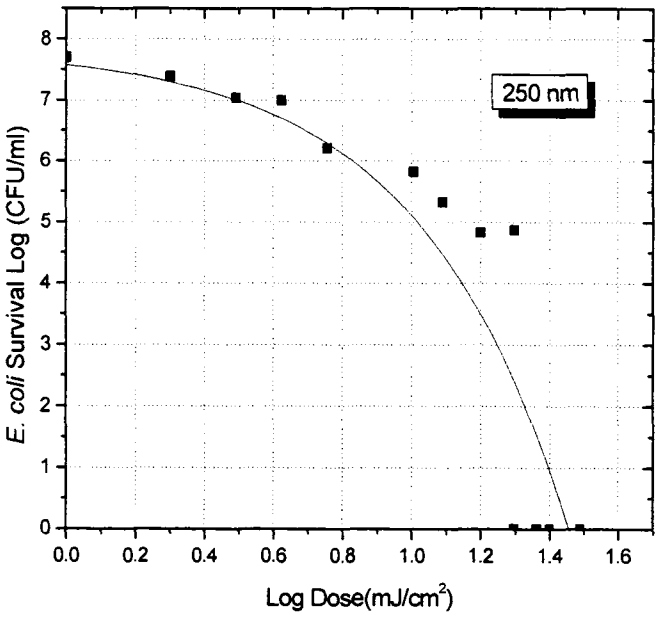

Figure 2. 6 - *E. coli* log survival vs. log dose at 250 nm. Parameter P_2=0.27451.

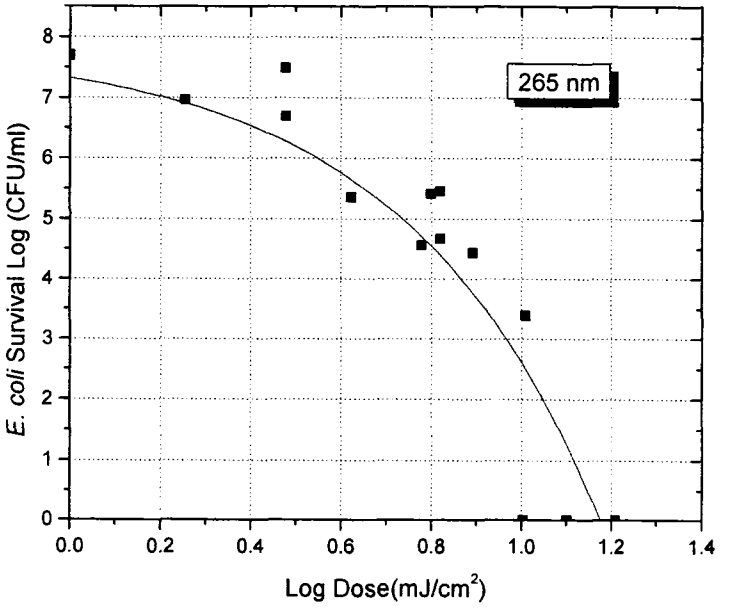

Figure 2. 7 - *E. coli* log survival vs. log dose at 265 nm. Parameter P_2=0.52329.

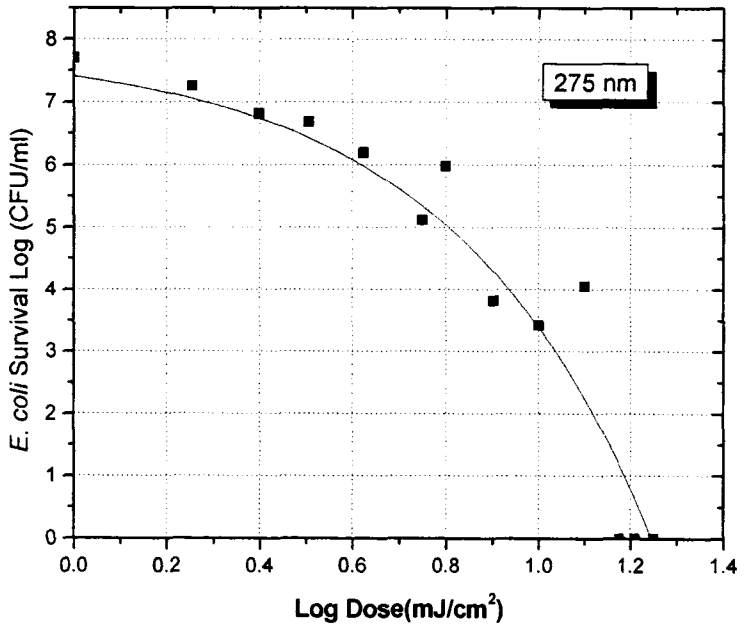

Figure 2. 8 - *E. coli* log survival vs. log dose at 275 nm. Parameter P_2=0.44537.

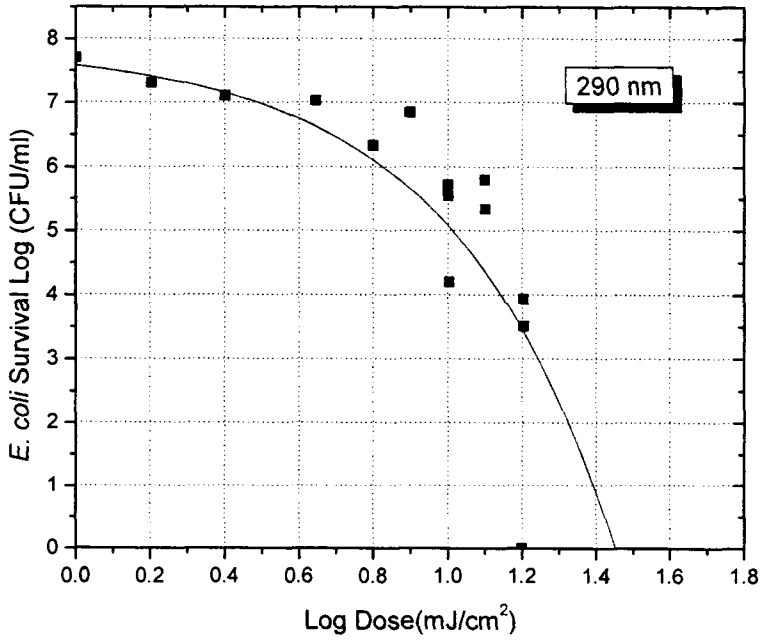

Figure 2. 9 - *E. coli* log survival vs. log dose at 290 nm. Parameter P_2=0.27691.

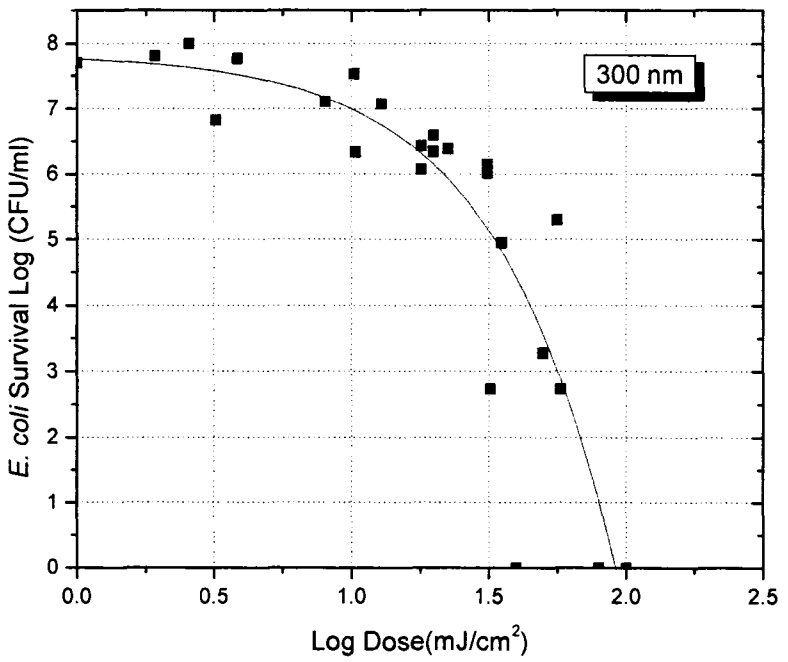

Figure 2. 10 - *E. coli* log survival vs. log dose at 300 nm. Parameter P_2=0.08587.

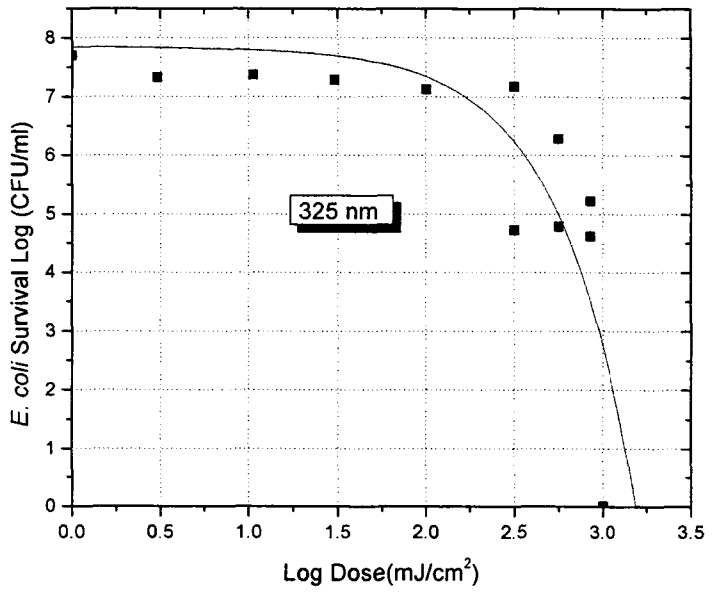

Figure 2. 11 - *E. coli* log survival vs. log dose at 325 nm. Parameter P_2=0.66802.

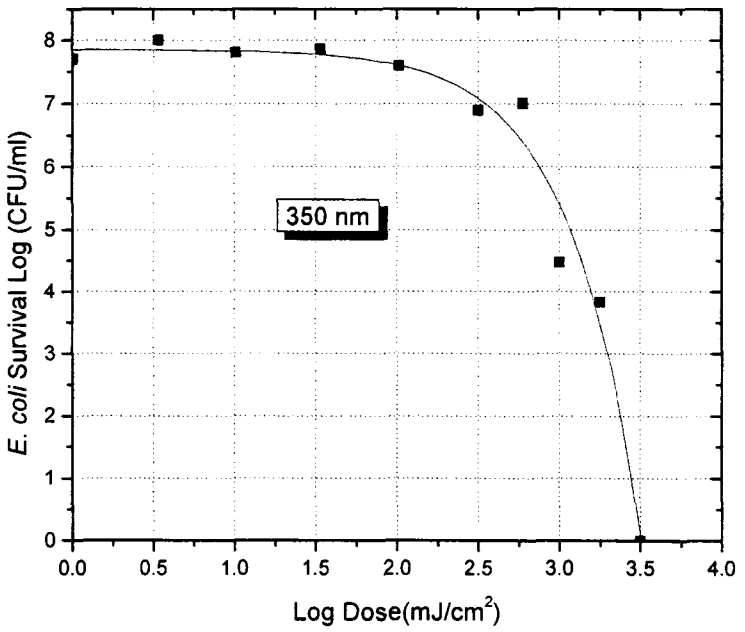

Figure 2. 12 - *E. coli* log survival vs. log dose at 350 nm. Parameter P_2=0.00245.

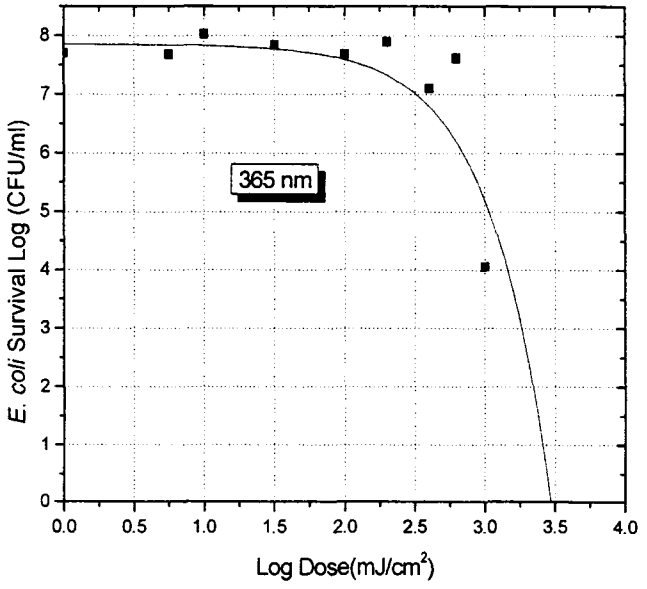

Figure 2. 13 - *E. coli* log survival vs. log dose at 365 nm. Parameter P_2=0.00265.

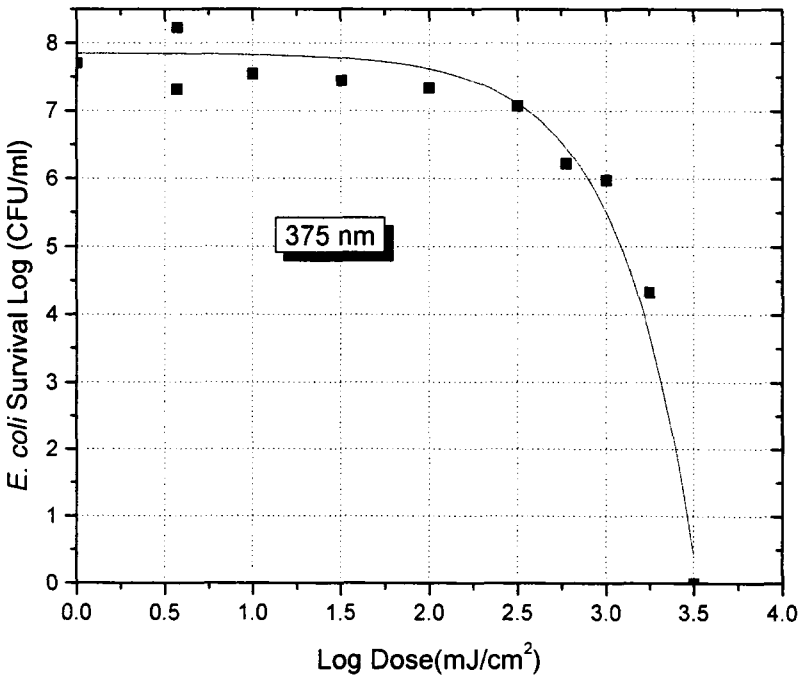

Figure 2. 14 - *E. coli* log survival vs. log dose at 375 nm. Parameter P_2=0.00234.

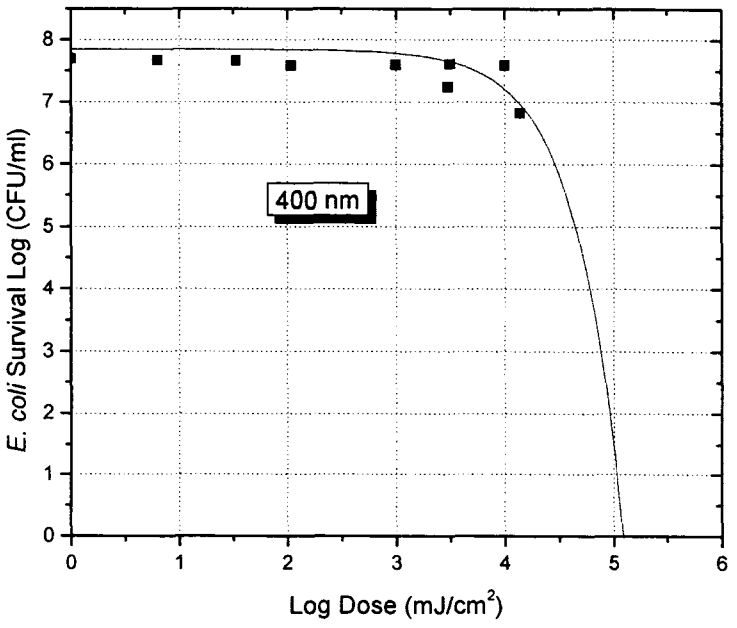

Figure 2. 15 - *E. coli* log survival vs. log dose at 400 nm. Parameter P_2=0.00006.

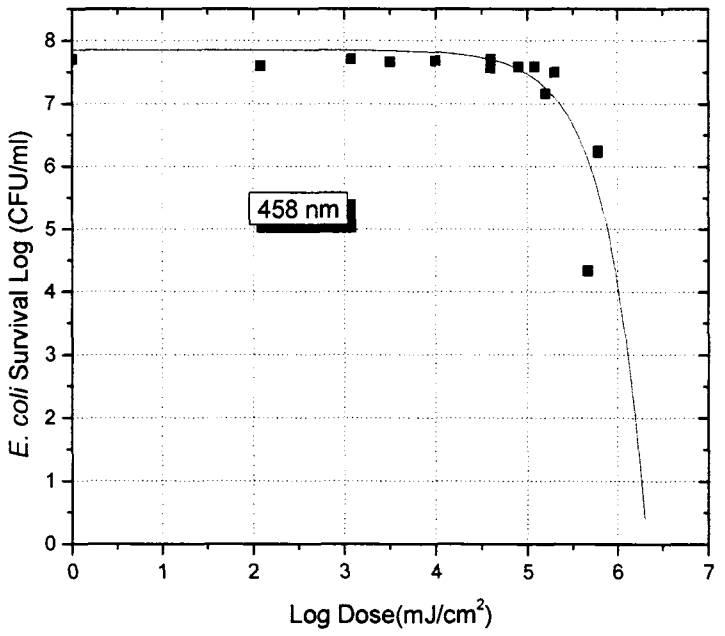

Figure 2. 16 - *E. coli* log survival vs. log dose at 458 nm. Parameter P_2=3.7314E-6.

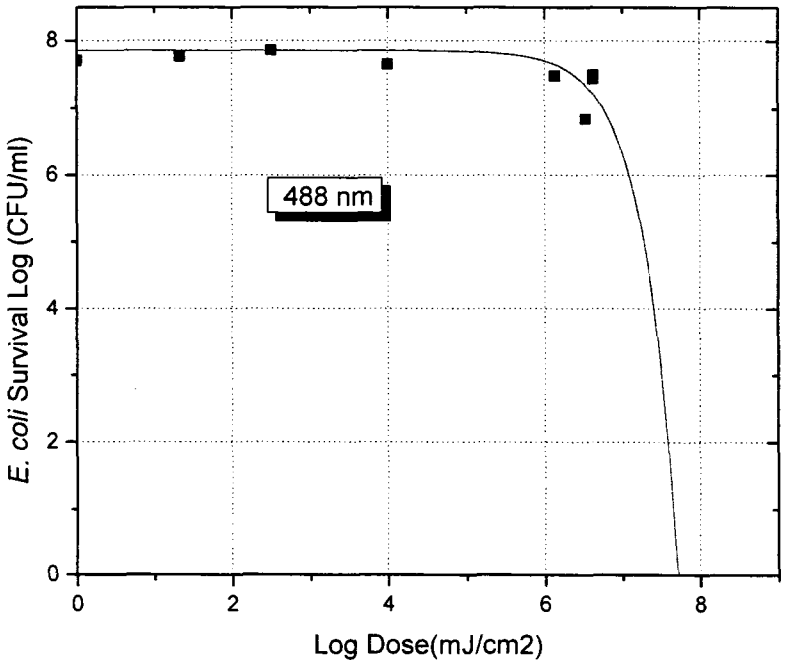

Figure 2. 17 - *E. coli* log survival vs. log dose at 488 nm. Parameter P_2=1.5106E-7.

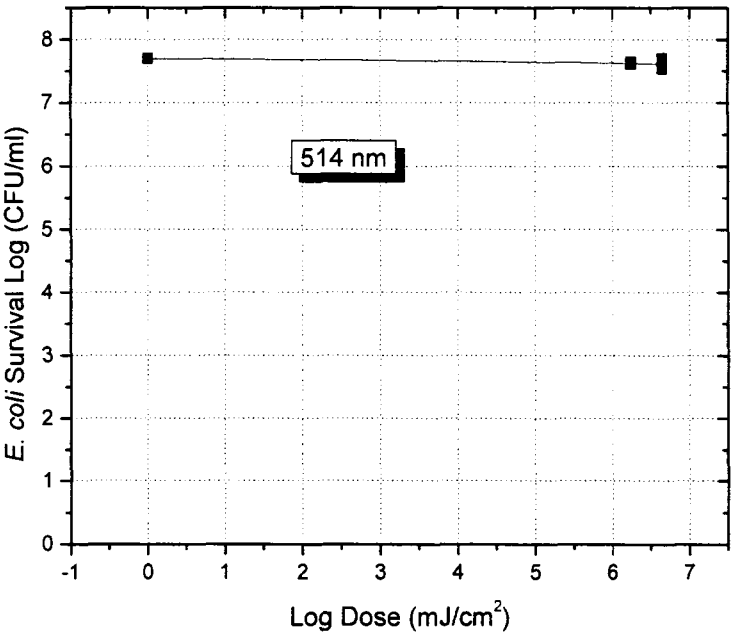

Figure 2. 18 - *E. coli* log survival vs. log dose at 514 nm.

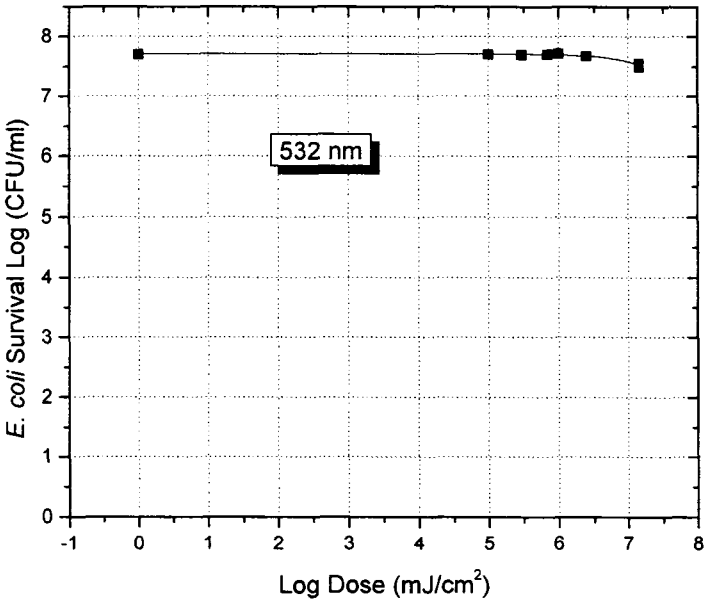

F

Figure 2. 19 - *E. coli* log survival vs. log dose at 532 nm.

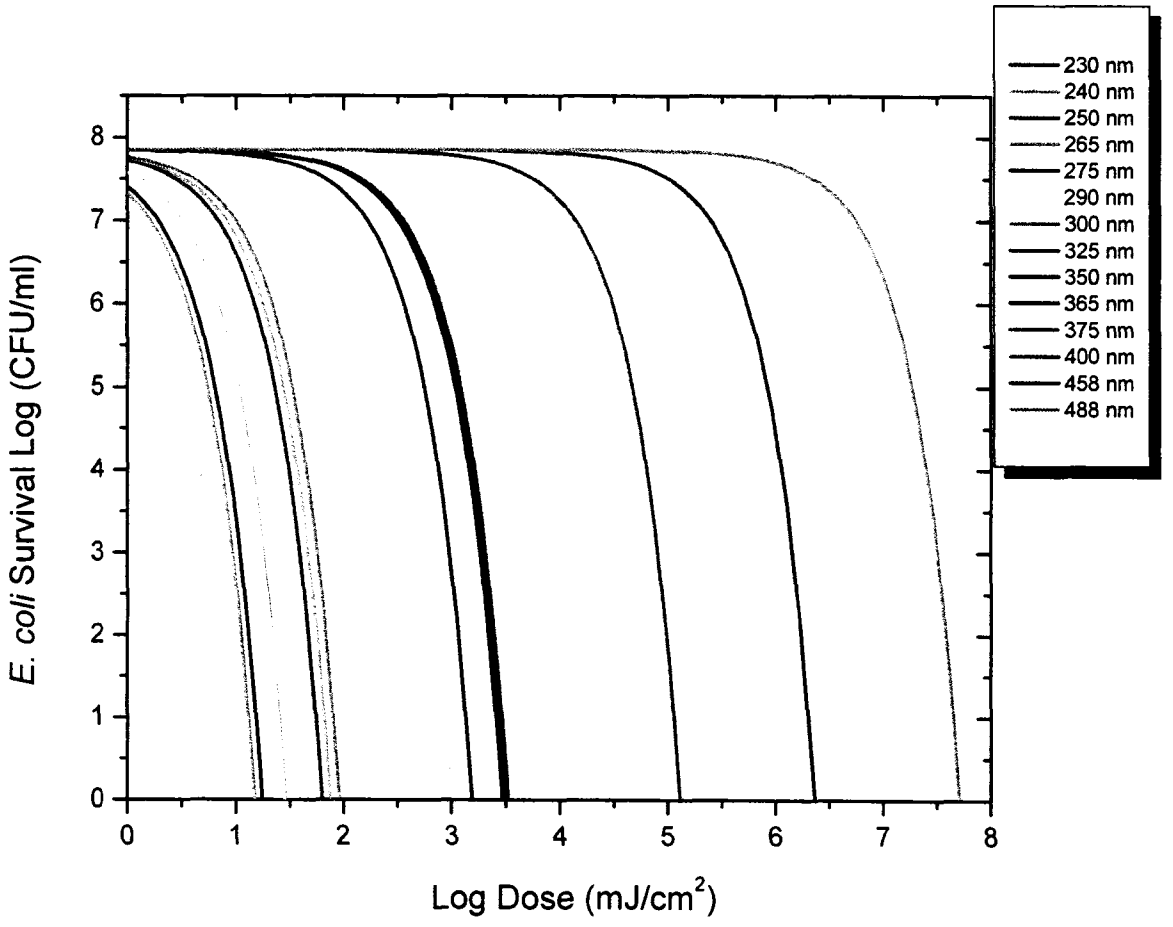

Figure 2. 20 - Best fit curves of all *E. coli* survival vs. dose wavelengths between 230 to 488 nm. The visible wavelengths 514 nm and 532 nm where not included because there was no kill observed at these wavelengths.

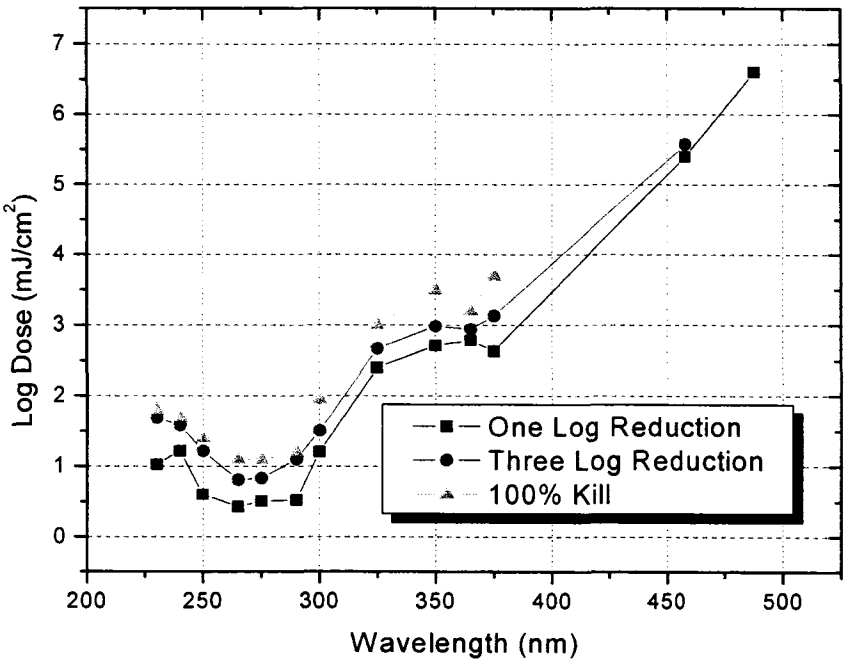

Figure 2. 21 - Log Dose vs. Wavelength *E. coli* kill curves.

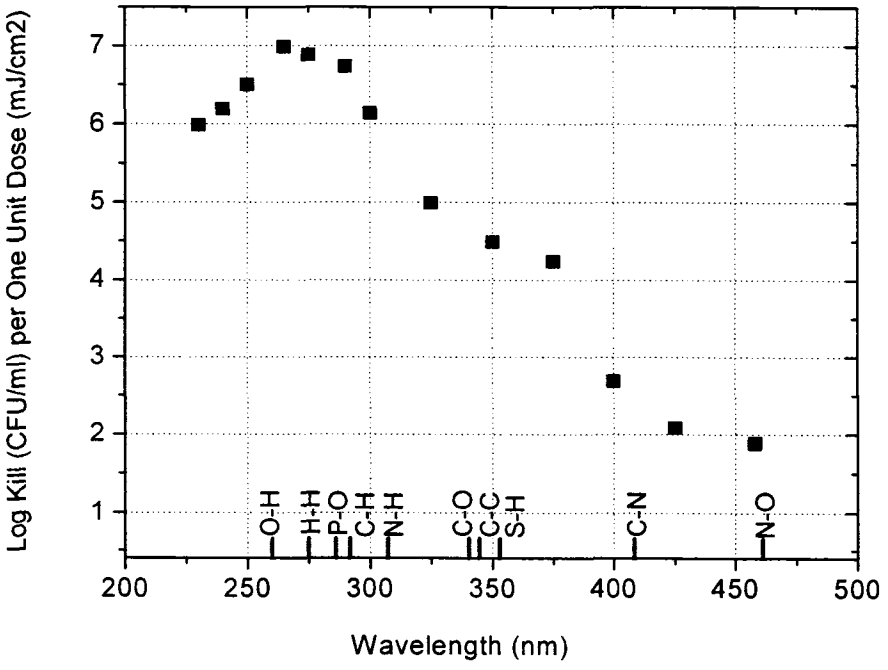

Figure 2. 22 - Log *E. coli* kill per one unit dose, with bond breaking energies at corresponding wavelengths.

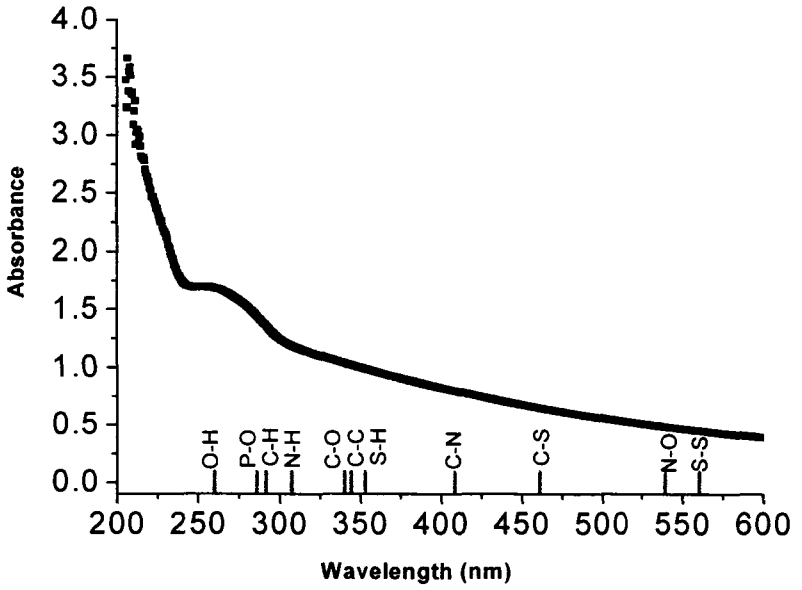

Figure 2. 23 - *E. coli* absorbances vs. wavelength, associated bond breaking energies are plotted at the appropriate wavelength.

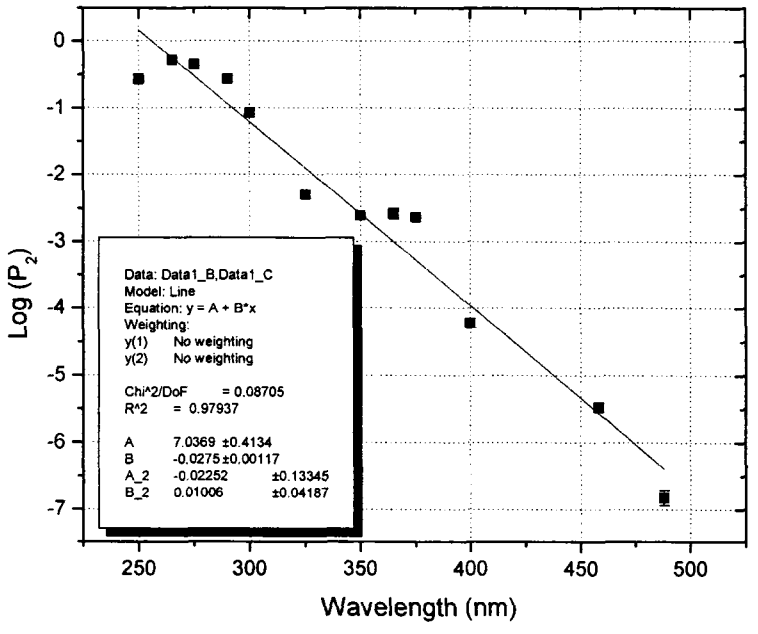

Figure 2. 24 - Curve fitting parameter P_2 vs. wavelength, points follow an exponential curve fit.

2.4 Discussion

The greatest number of bacteria killed per one unit of dose occurred between 260 – 280 nm. It is apparent that the peak of the killing curve in Figure 2.22 coincides with the absorption peak of the UV – visible absorption spectrum of the *E. coli* cells (Figure 2.23). From our calculation of the equivalent photon wavelengths (Table 2.2), for the most important biomolecular bondings, such as O–H, P–O, and N–H bonds, it is apparent these are susceptible to breakage by UV radiation at around 260 – 280 nm. Since P–O bonds are a part of the backbone structure of nucleic acids (Becker et al., 2003) and the O–H and N–H bonds are essential to the hydrogen bonds that maintain tertiary structure of proteins and DNA (Lodish et al., 1994). This may explain the high killing capability of UV at around 270 nm and the UV absorption peak around 260 – 280 nm. Another explanation for the decrease in the killing capacity of UV at wavelengths less than 265 nm may be due to the exponential increase in UV absorption of water at wavelengths less than 250 nm

Total kills were not obtained in the visible light section, but there was significant killing observed at the 458 and 488 nm laser lines (Figure 2.16 and 2.17) after very high photon fluxes (doses) were delivered. The high photon fluxes were required because only the low energy C-S, N-O, and S-S bonds (Table 2.2) could be broken and these are apparently less important to the survival process. However, for the longer visible light wavelengths, 514nm and 532nm, no significant kill was observed (Figure 2.18 and Figure 2.19). Photon energy at these wavelengths can no longer break the C-S bonds which are presumably more important than the N-O and S-S bonds. Using the graph in Figure 2.22, one obtains an estimate of the required lethal dose at about 20,000,000

mJ/cm^2 for 532 nm. At high intensity, a visible laser could inflict heat damage on the bacterium causing cell death. However, this was not tested in this study because temperature increases were kept below ~1 C in all sample runs. Despite the fact that UV light irradiation has been used as a disinfectant for decades, there has not been a predictive model reported to quantify the killing capacity of radiation at various wavelengths. However, based on the *E. coli* survival data at various wavelengths and dosages obtained during this study, an equation has been proposed (Equation 2.6) that generally predicts the mortality of *E. coli* from ~250nm to 500 nm, and over a change in dose of seven orders of magnitude. Further, it is speculated that the rapid variation in the mortality (exponential in dose and double exponential in wavelength) is due to the direct effect that bond breaking photons have on the photochemistry of the biochemical organisms. At present though, a complete model of the biological changes induced by the light, can not be offered. In order to try to obtain further information on the possible biochemical effects induced by the light, a spectroscopic investigation of UV exposed *E. coli* was initiated. This is further discussed in the next Chapter.

Chapter 3: ATR-FTIR Spectroscopy of UV Treated *E. coli*

3.1 Introduction

Since UV is so widely used as a bactericidal agent (Decho, 2000; Hamblin, 2005), it is important to understand the mechanisms in which UV damages bacterial cells. When bacteria are exposed to UV radiation, the high energy radiation can initiate photochemical reactions that involve breaking chemical bonds of biomolecules, causing the formation of harmful byproducts. For example, cyclobutane-pyrimidine and pyrimidine-pyrimidone dimers are common UV-induced byproducts that cause mutation to microorganisms (Hader and Sinha, 2005). UV also creates reactive oxygen species (ROS) such as superoxide anion, hydrogen peroxide and singlet oxygen which cause oxidative damages to cellular components (Becerra et al., 2004).

Some techniques are available to assess UV damages to bacterial cells. For example, to determine the increase in ROS production, there are different procedures at hand. Such procedures include determining the increase of ROS by measuring the oxidation of Nitro Blue Tetrazolium (NBT) (Becerra et al., 2004) and the decrease of cytochrome c (Godley et al., 2005). There are numerous ways to detect the DNA damage inflicted by ROS. One example is to measure the increase of 8-hydroydeoxyguanosine (generated by oxidative damage of DNA) (Schriner et al., 2005). However, most of these assays are designed to quantify a specific group of UV affected chemicals, which indicate a specific type of UV damage. None of these assays shows the effect of UV on the overall changes of biomolecules in bacterial cells.

FTIR can be used to analyze the types and the relative amount of chemical bonds that are present in a complex organic sample (Hirschmugl, 2004). It is useful for variety of sample matrixes, such as: liquids, pastes, powders, films, gases, fibers and many different kinds of solid surfaces (Stuart, 1996). When a specific wavelength of IR radiation interacts with a sample, it will be absorbed by a specific chemical bond causing the chemical bond to vibrate (Smith, 1996). The IR spectrum of a sample represents the chemical bonding fingerprint of the sample (Hirschmugl, 2004). Furthermore, the signal to noise ratio of the FTIR assay can be increased significantly by using an attenuated total reflectance (ATR) sampler (Christy et al., 2001). Therefore, the ATR-FTIR analysis is well suited for examining the overall changes of bacterial cells at the molecular structure level. In the previous chapter, we showed that UV radiation between 260-280 nm was most efficient in causing mortality to *E. coli* cells. The objective of this chapter is to use the ATR-FTIR method to examine the effect of UV on *E. coli* at the molecular level.

3.2 Materials and Methods

3.2.1 ATR-FTIR Spectrophotometer

ATR-FTIR spectroscopy was used to assess the different chemical bondings present in the UV treated and untreated *E. coli* samples. The FTIR in this experiment was a Bruker Tensor 37 FTIR. The ATR accessory was a MiRacle ATR from PIKE technologies (2901 Commerce Park Drive, Madison, WI 53719). The ATR used in this study had a ZnSe crystal and was fixed with a 0-8 pound pressure clamp.

3.2.2 Bacteria Preparation and UV Treatment

Escherichia coli ATCC 25922, a Gram-negative bacterium, was obtained from the American Type Culture Collection (ATCC). *Enterococcus faecalis* ATCC 29212 is a Gram - positive bacterium. The *Pseudomonas* strain (previously classified as a *Moraxella* strain) used in this study was obtained form an active sludge environment (Spain and Gibson, 1991). The *E. coli* ATCC 25922 and *E. faecalis* ATCC 29212 were cultured in sterile Tryptic Soy Broth (TSB) for 15h, with shaking at 150 rpm, at 37°C. The *Pseudomonas* strain was cultured in sterile TSB for 15h, with shaking at 150 rpm, at 30°C. After incubation, all bacterial cultures were washed 3x in sterile distilled water and suspended in sterile distilled water at an OD_{600} of 0.30 (about 10^8 CFU/ml). However, only the *E. coli* sample was treated with UV radiation in this study. One hundred µl of the *E. coli* suspension was placed in a ring device for UV treatment as described in the previous chapter. A sub-sample of the *E. coli* suspension was used for an experimental control that did not receive the UV treatment. In this study, only 275 nm UV light was used to treat samples, and the dose was set at about 3x the lethal dose (1.2 mJ/cm^2) of that wavelength.

3.2.3 ATR-FTIR analysis

Because water has a high absorbance of IR radiation, complete drying of the bacterial cells by lyophilization was necessary. To prepare the sample for lyophilization, 2 ml of UV treatment of *E. coli* was centrifuged for 5 minutes at 3100 x *g*. Excess water was removed from the cell pellet and the pellet was mixed with 4ml of 5% dimethylsulphoxide (DMSO) aqueous solution to preserve the cells during lyophilization. The *E. coli* suspension was placed into sterile glass vials with a sterilized cotton closure.

The cell samples were rapidly frozen in liquid nitrogen and the frozen samples were placed into to a lyophilizer and dried for two days. The lyophilized samples were placed on the ZnSe crystal holder in the ATR-FTIR, analyzed, and the corresponding IR spectra were produced.

3.3 Results and Discussion

To examine the sensitivity of the ATR-FTIR assay, Mid-IR spectra of the *E. coli* ATCC 25922 strain, *E. faecalis* ATCC 29212 strain, and a *Pseudomonas* strain was compared. Figure 3.1a and b show that the ATR-FTIR assay detected all the major cellular molecular components of the 3 bacterial species as described in other studies (Naumann, 2000). For instance, the spectral region between 900-1200cm^{-1} represents the symmetric stretching vibrations of C-O-P and P=O of nucleic acids and C-O-C of polysaccharides (cell wall and polysaccharide capsule structures). The major peak at 1230 cm^{-1} represents asymmetric stretching vibration of P=O groups of nucleic acids. Other major absorption peaks such as 1400, 1450, 1550, 1670, 3100-2800, 3250 and 3400 cm^{-1} represents $-COO^-$, CH_2, N-H of amide, C=O of amide, C=C of fatty acids and lipids, N-H of proteins and O-H stretching of hydroxyl groups, respectively (Naumann, 2000). Figure 3.1b also shows that the intensity ratios of the C-O-C peak (900-1200 cm^{-1}) to P=O peak (1230 cm^{-1}) of the 3 bacterial strains are substantially different from each other. The *E. faecalis* had the highest C-O-C: P=O ratio. The *Pseudomonas* strain was the second and the *E. coli* had the lowest ratio. This agrees with the fact that *E. faecalis* is a Gram - positive bacteria, which has the highest amount of cell wall (i.e., C-O-C bending). *Pseudomonas* species is well known to produce a large amount of

capsular polysaccharides and this may attribute to the higher C-O-C : P=O ratio of the *Pseudomonas* strain.

Having shown that our ATR-FTIR protocol was sufficient to detect differences between molecule structures and/or components of various bacterial species, we used the ATR-FTIR assay to examine the effect of UV on the cellular molecular composition of the *E. coli* ATCC 25592. Figure 3.2a illustrates the IR spectra of the UV- treated and the untreated *E. coli*. Figure 3.2b and 3.2c show the IR absorbance ratios of the UV-treated and untreated *E. coli* cells in two independent FTIR trials, showing reproducible outcomes of the two trials. Figure 3.2d represents the average IR absorbance ratios of the UV-treated and untreated cells, showing several major molecular changes on the UV-exposed *E. coli* cells. For instance, a significant decrease of absorbance between 900-1200 cm^{-1} was observed for the UV-treated *E. coli* samples. This indicated a decrease of C-O-C, C-O-P, and/or P=O bonding after UV-treatment, indicating destruction of the glycan backbone of peptidoglycan and the phosphodiester backbone of nucleic acids. This observation agrees with other studies that UV can affect the cell wall (Eisenstark, 1987) and adhesion of bacterial cells (Nanadakumar et al., 2006). UV is also known to degrade nucleic acids by breaking their phosphodiester bonds. Despite the well known fact that UV will break down nucleic acids (Hader and Sinha, 2005), a decrease of the 1230 cm^{-1} peak, representing the P=O of nucleic acids, was not detected on the UV-treated samples. This infers that UV is involved in breaking the P-O-C bond (at 900-1200 cm^{-1}) but not the P=O bond (at 1230 cm^{-1}) of nucleic acids.

In contrast to nucleic acids and carbohydrates, there was an increase in protein content in the UV-treated samples. This can be observed in Figure 3.2d, that there are

significant increases in peaks at 1550, 1670 and 3280 cm^{-1}, representing the N-H and C=O of the amide I and amide II bonds, and N-H stretching of amide bonding of proteins, respectively. The increase in cellular proteins may be a stress response mechanism of the *E. coli* cells exposed to the UV treatment. Storz and Hengge-Aronis (2000) showed that a SOS-like response was initiated in bacterial cells after UV irradiation. This may explain the increase in protein content of the UV-treated *E. coli* cells in our experiment.

The UV treated cells also showed an increase in the amount of CH_2 stretching of fatty acids (between 2800-3100 cm^{-1}), indicating a change in membrane structure of the UV treated bacteria (Alberts, 1994). Furthermore, the increase in the hydroxyl groups (3400 cm^{-1}) on the UV-treated samples may reflect an increase of reactive oxidation species (ROS) in the *E. coli* cells. For example, the hydroxyl radical (·OH) has been shown to damage cellular components, such as DNA, RNA, proteins and lipids, forming hydroxyl derivatives (Pomposiello et al., 2000).

In conclusion, the ATR-FTIR assay was able to reveal several molecular changes in the UV treated *E. coli* cells. Besides the predicted decrease in nucleic acids and increase in hydroxyl derivatives, interesting observations such as the increase in proteins and fatty acids deserve further investigation because the cellular changes may have implications to the stress survival response mechanisms of bacteria against UV radiation.

Figures

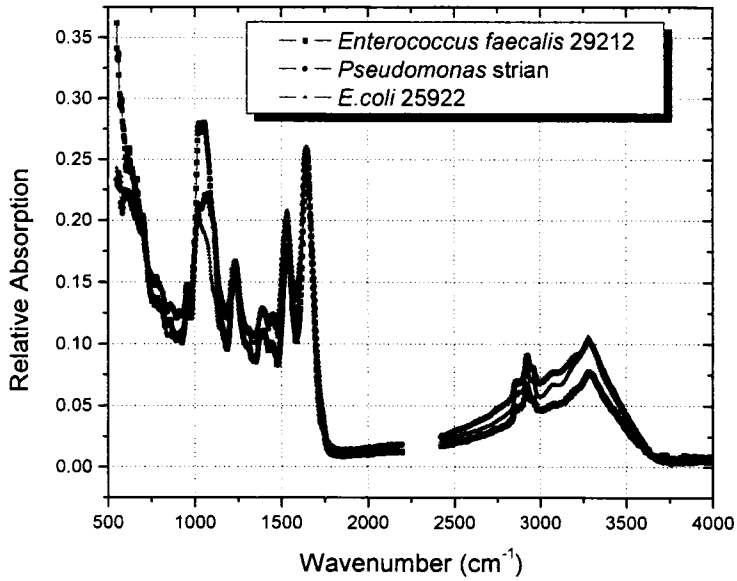

(a)

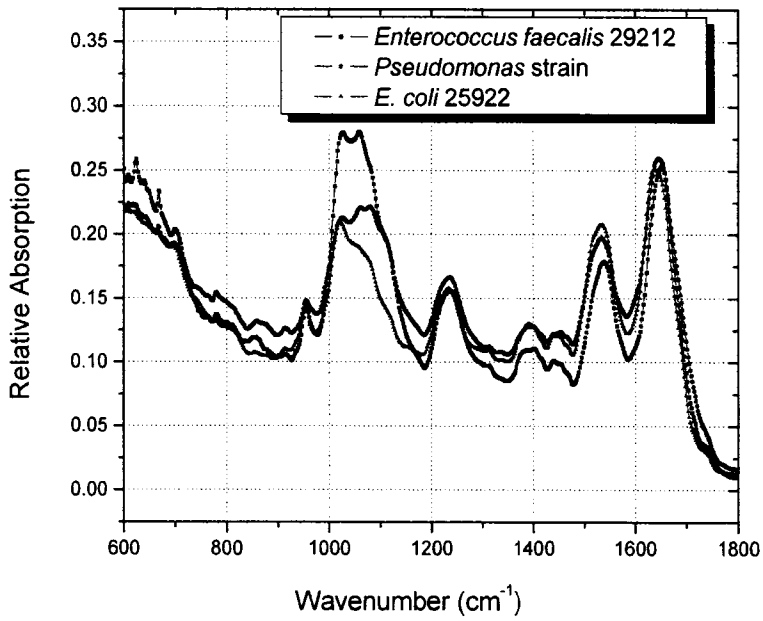

(b)

Figure 3. 2 - (a) IR spectra of three different bacteria showing different peak intensities. (b) Expanded view from 600 to 1800 cm^{-1}. Note major differences around 1000 cm^{-1}.

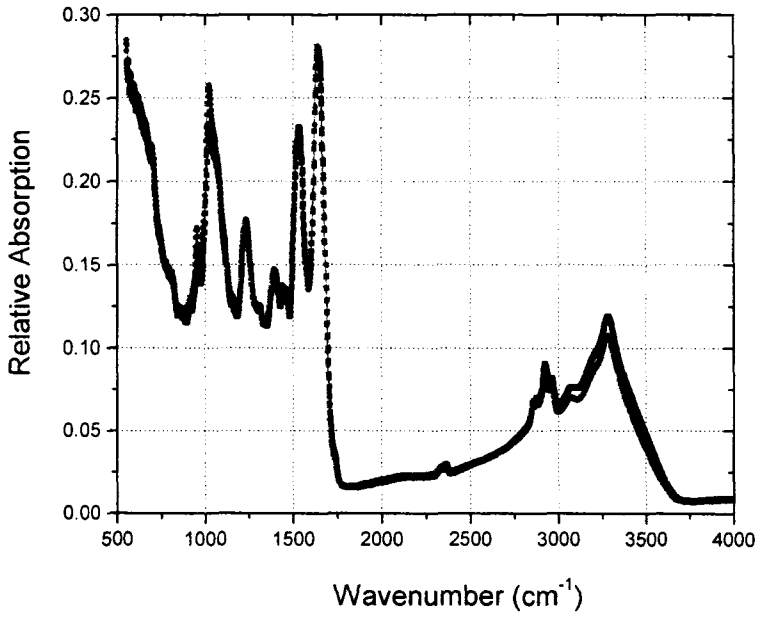

Figure 3. 2a - ATR-FTIR Spectrum of untreated *E. coli* (red) and *E. coli* treated (black).

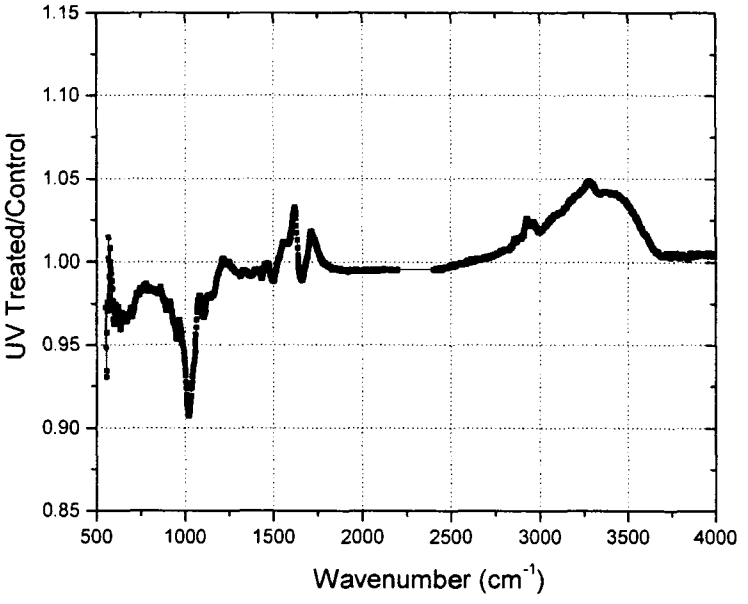

Figure 3. 2b – Ratio of UV treated *E. coli* to untreated *E. coli* (first replication).

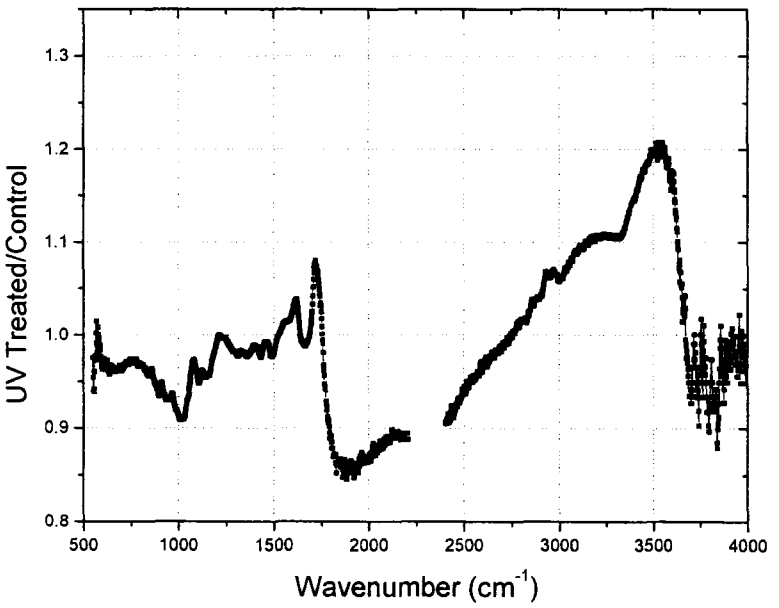

Figure 3. 2c - Ratio of UV treated *E. coli* to untreated *E. coli* (second replication).

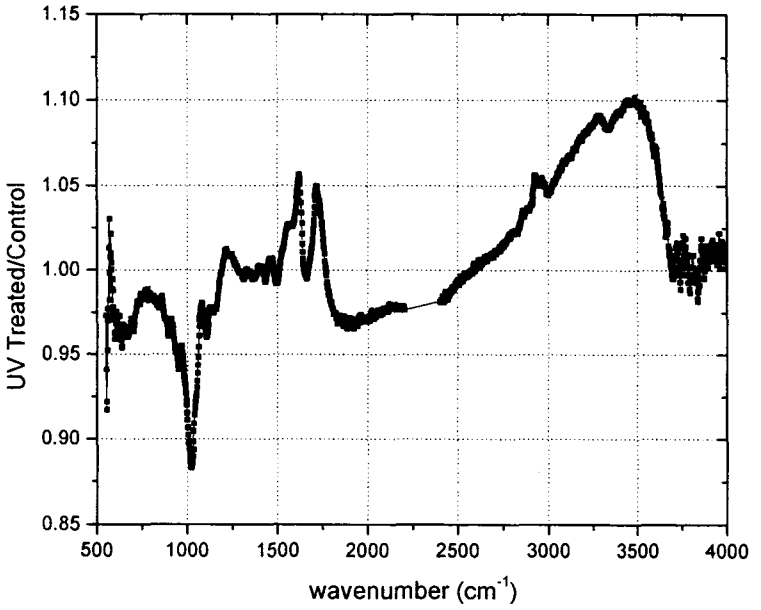

Figure 3. 2d – Average of Figure 3.2b and 3.2c.

References

Alberts, B., Dennis, B., Lewis, J., Raff, M., Roberts, K. and Watson, J.D. 1994. Molecular Biology of the Cell. New York and London: Garland Pubishing, Inc. pp1294.

Becerra, M.C., Sarmiento, M., Paez, P.L., Arguello, G. and Albesa, I. 2004. Light effect and reactive oxygen species in the action of ciprofloxacin on *Staphylococcus aureus.* Journal of Photochemistry and Photobiology B: Biology. **76**: 13-18.

Becker, W.M., Klleinsmith, L.J. and Hardin, J. 2003. The World of the Cell. San Francisco, CA: Benjamin Cummings. pp 802.

Ben-Hur, E. and Petrie, T. 2004. Ultraviolet light irradiation (UBI) for the treatment of chronic hepatitis C patients: preclinical studies. Proc. 32nd Annual Meeting, American Society for Photobiology, p. 58.

Betts, G.D. 2000. Controlling *E. coli* 0157. Nutrition and Food Science. **30**: 183-186.

Burger, A., Raymer, J. and Bockrath, R. 2002. DNA damage-processing in *E. coli*: on-going protein synthesis is required for fixation of UV-induced lethality and mutation. DNA Repair. **1**: 821-831.

Carell, T., Burgdorf, L.T., Kundu, L.M., and Cichon, M. 2001. The mechanism of action of DNA photolyases. Current Opinion in Chemical Biology. **5**: 491-498.

Cartier, R.H. 2004. Seeing the Light. Canada: Archives Canada Cataloguing in Publication. pp 324.

Chang, J.C., Ossoff, S.F., Lobe, D.C., Dorfman, M.H., Dumais, C.M., Qualls, R.G., and Johnson, J.D. 1985. UV inactivation of pathogenic and indicator microorganisms. Applied and Environmental Microbiology. **49**: 1361-1365.

Christy, A.A. Ozaki, Y. and Gregoriou, V.G. 2001. Modern Fourier: Transform Infrared Spectroscopy. Amsterdam: Elsevier Science B.V. pp 356.

Crummett, W.P. and Western. 1994. University Physics Models and Applications. Wm. C. Brown Publishers. pp. 1224.

Deborah Chen, H., and Frankel, G. 2005. Enteropathogenic *Escherichia coli*: unraveling pathogenesis. FEMS Microbiology Reviews. **29**: 83-98.

Decho, AW. 2000. Microbial biofilms in intertidal systems: an overview. Continental Shelf Researh. **20:** 1257-1273.

Devine, D.A., Keech, A.P., Wood, D.J., Killington, R.A., Boyes, H., Doubleday, B., and

Marsh, P.D. 2001. Ultraviolet disinfection with a novel microwave-powered device. Journal of Applied Microbiology. **91**: 786-794.

Dougherty, T.J. 2002. An update on photodynamic therapy applications. Journal of Clinical Laser Medicine and Surgery. **20**: 3-7.

Eisenstark, A. 1987. Mutagenic and lethal effects of near-ultraviolet radiation (290-400nm) on bacteria and phage. Environmental and Molecular Mutagenesis. **10**: 317-337.

Eisenstark, A. 1971. Mutagenic and lethal effects of visible and near-ultraviolet light on bacterial cells. Advances in Genetics. **16**: 167-198.

Elman, M., Slatkine, M and Harth, Y. 2003. The effective treatment of *acne vulgaris* by a high-intensity, narrow band 405-420nm light source. Journal of Cosmetic and Laser Therapy. **5**: 111-117.

Folwaczny, M., Liesenhoff, T., Lehn, N. and Horch, H-H. 1998. Bactericidal action of 308nm excimer-laser radiation: An in vitro investigation. Journal of Endodontics. **24**: 781-785.

Gates, F.L. 1929. A study of the bactericidal action of ultra violet light: I. The reaction of monochromatic light. The Journal of General Physiology. **13**: 231-248.

Gates, F.L. 1929. A study of the bactericidal action of ultra violet light: II. The effect of various environmental factors and conditions. The Journal of General Physiology. **13**: 249-260.

Gates, F.L. 1930. A study of the bactericidal action of ultra violet light: III. The absorption of ultra violet light by bacteria. The Journal of General Physiology. **14**: 31-42.

Godley, B.F., Shamsi, F.A., Linang, F., Jarret, S.G., Davies, S., and Boulton, M. 2005. Blue light induces mitochondrial DNA damage and free radical production in epithelial cells. The Journal of Biological Chemistry. **280**: 21061-21066.

Griffiths, H. 1986. Fourier Transform Infrared Spectrometry. Chichester: John Wiley and Sons Ltd. pp 656.

Hader, D.P. and Sinha, R.P. 2005. Solar ultraviolet radiation-induced DNA damage in aquatic organisms: potential environmental impact. Mutation Research. **571**: 221-233.

Hamblin, M.R., Viveiros, J., Yang, C., Ahmadi, A., Ganz, R.A. and Joshua Tolkoff, M. 2005. *Helicobacter pylori* accumulates photoactive porphyrins and is killed by visible light. Antimicrobial Agents and Chemotherapy. **49**: 2822-2827.

Heck, D.E., Vetrano, A.M., Mariano, T.M., and Laskin J.D. 2003. UVB light stimulates production of reactive oxygen species. The Journal of Biological Chemistry. **278**: 22432-22436.

Hirschmugl, C. 2004. An Introduction to Infrared Spectroscopy for Geochemistry and Remote Sensing. In: King, P.L., Ramsey, M.S. and Swayze, G.A., editor. Infrared Spectroscopy in Geochemistry, Exploration Geochemistry, and Remote Sensing. London, Ontario: Mineralogical Association of Canada. pp 1-16.

Hockberger, P.E. 2002. A history of ultraviolet photobiology for humans, animals and microorganisms. Photochemistry and Photobiology. **76**: 561-579.

Jagger, J. 1976. Effects of near-ultraviolet radiation on microorganisms. Photochemistry and Photobiology. **23**: 451-454.

Jones, E.R. and Childers, R.L. 1993. Contemporary Collage Physics. Menlo Park, California: Addison-Wesley Publishing Company. pp 941.

Kuhnert, P., Boerlin, P., and Frey, J. 2000. Target genes for virulence assessment of *Escherichia coli* isolates from water, food and the environment. FEMS Microbiology Reviews. **24**: 107-117.

Lidwell, O.M. 1994. Ultraviolet radiation and the control of airborne contamination in the operating room. Journal of Hospital Infection. **28**: 245-248.

Lodish, H., Baltimore, D., Berk, A., Zipursky, S.L., Matsudaira, P. and Darnell, J. 1995. Molecular Cell Biology. New York, New York: Scientific American Books, Inc. pp 1344.

Lowell, J.D. and Pierson, S.H. 1989. Ultraviolet irradiation and laminar air flow during total joint replacement. In: Kundsin RB, Ed. Architectural Design and Indoor Microbial Pollution. New York: Oxford Press.

Madigan, M.T., Martinko, J.M., and Parker, J. 2000. Brock Biology of Microorganisms. Upper Saddle River, NJ: Prentice Hall. pp 991.

Moan, J. 1989. Effects of UV radiation on cells. Journal of Photochemistry and Photobiology, B: Biology. **4**: 21-34.

Moore, C.M., Hoh, I.M., Bown, S.G., and Emberton, M. 2005. Dose photodynamic therapy have the necessary attributes to become a future treatment for organ-confined prostate cancer? BJU International. **96**: 754-758.

Nanadakumar, K., Obika, H., Shinozaki, T., Ooie, T., Utsumi, A., and Yano, T. 2003. Laser impact assessment in a biofilm-forming bacterium *Pseudoalteromonas*

carrageenovora using a flow cytometric system. Biotechnology and Bioengineering. **82**: 399-402.

Nanadakumar, K., Obika, H., Shinozaki, T., Ooie, T., Utsumi, A., and Yano, T. 2003. Laser impact on bacterial ATP: Insights into the mechanism of laser-bacteria interactions. Biofouling. **19**: 109-114.

Nanadakumar, K., Obika, H., Shinozaki, T., Ooie, T., Utsumi, A., and Yano, T. 2003. Laser impact on marine planktonic diatoms: an experimental study using a flow cytometry system. Biofouling. **19**: 133-138.

Nanadakumar, K., Obika, H., Shinozaki, T., Ooie, T., Utsumi, A., and Yano, T. 2003. Pulsed laser irradiation impact on two marine diatoms *Skeletonema costatum* and *Chaetoceros gracilis*. Water Research. **37**: 2311-2316.

Nanadakumar, K., Obika, H., Shinozaki, T., Ooie, T., Utsumi, A., and Yano, T. 2002. Impact of pulsed Nd:YAG laser irradiation on the growth and mortality of the biofilm forming marine bacterium *Pseudoalteromonas carrageenovora*. Biofouling. **18**: 123-127.

Naumann, D. 2000. Infrared Spectroscopy in Microbiology. In: Meyers, R.A., editor. Encyclopedia of Analyical Chemistry. Chichester: John Wiley and Sons Ltd. pp. 102-131.

Prasad, K., Laxdal, V.A., Yu, M., and Raney B.R. 1995. Evaluation of hydroxyl radical-scavenging property of garlic. Molecular and Cellular Biochemistry. **154**: 55-63.

Richter, A., Mahmoud, S.A. and Ries, R. 2002. Changes of biofilm structures on polymer substrates caused by laser beams. Vacuum. **66**: 179-188.

Salyers, A.A. and Whitt, D.D. 2002. Bacterial Pathogenesis a Molecular Approach. Washington, DC: ASM Press. pp 539.

Schriner, S.E., N.J. Linford, G.M. Martin, P. Treuting, C.E. Ogburn, M. Emond, P.E. Coskun, W. Ladiges, N. Wolf, H. van Remmen, D.C. Wallace, and P.S. Rabinovitch. 2005. Extension of Murine life span by overexpression of catalase targeted to mitochondria. Science **308**: 1909 -1911.

Schwartz, T., Hoffmann, S., and Obust, U. 2003. Formation of natural biofilms during chlorine dioxide and UV disinfection in a public drinking water distribution system. Journal of Applied Microbiology. **95**: 591-601.

Sharrer, M.J., Summerfelt, S.T., Bullock, G.L., Gleason, L.E., and Taeuber, J. 2005. Inactivation of bacteria using ultraviolet irradiation in a recirculating salmonid culture system. Aquacultural Engineering. **33**: 135-149.

Sinha, R.P. and Hader, D.P. 2002. UV-induced DNA damage and repair: a review. Photochemistry and Photobiology Society. **1**: 225-236.

Smith, B.C. 1996. Fourier Transform Infrared Spectroscopy. Boca Raton, Florida: CRC Press. pp 202.

Storz, G. and Hengge-Aronis, R. 2000. Bacterial Stress Responses. Washington, DC: ASM Press. pp 485.

Stuart, B. 1996. Modern Infrared Spectroscopy. Chichester, England: John Wiley and Sons. Ltd. pp 180.

Szpringer, E., Lutnicki, K. and Marciniak, A. 2004. Photodynamic therapy—mechanism and employment. Annales Universitantis Mariae Curie-Sk inverted question markodowska. Sectio D: Medicina. **59**: 498-502.

Thomas, G. 1977. Effects of Near Ultraviolet Light on Microorganisms. Photochemistry and Photobiology. **26**: 669-673.

Tuteja, N. and Tuteja, R. 2001. Unraveling DNA repair in human: Molecular mechanisms and consequences of repair defect. Critical Reviews in Biochemistry and Molecular Biology. **36**: 261-290.

Van Houdt, R., and Michiels, C.W. 2005. Role of bacterial cell surface structures in *Escherichia coli* biofilm formation. Research in Microbiology. **156**: 626-633.

Weber, S. 2005. Light-driven enzymatic catalysis of DNA repair: a review of recent biophysical studies on photolyase. Biochimica et Biophysica Acta. **1701**: 1-23

Wei, H., Ca, Q., Rahn, R., Zhang, X., Wang, Y. and Lebwohl, M. 1998. DNA structural integrity and base composition affect ultraviolet light-induced oxidative DNA damage. Biochemistry. **37**: 6485-6490.

Wilson, M. 1994. Bactericidal effect of laser light and its potential use in the treatment of plaque-related diseases. International Dental Journal. **44**: 181-189.

Zumbahl, S.S. 1997. Chemistry. Boston, MA: Houghton Mifflin Company. pp 1118.